JVI Journals.ASM.org

Functional Characterization of Bovine Viral Diarrhea Virus Nonstructural Protein 5A by Reverse Genetic Analysis and Live Cell Imaging

Olaf Isken,[a,c] Ulrike Langerwisch,[a,c] Robert Schönherr,[b,c] Benjamin Lamp,[d] Kristin Schröder,[a,c] Rainer Duden,[b,c] Tillmann H. Rümenapf,[d] Norbert Tautz[a,c]

Institute of Virology and Cell Biology[a] and Institute of Biology,[b] Center of Structural and Cell Biology in Medicine,[c] University of Lübeck, Lübeck, Germany; Institute of Virology, University of Veterinary Medicine, Vienna, Austria[d]

Nonstructural protein 5A (NS5A) of bovine viral diarrhea virus (BVDV) is a hydrophilic phosphoprotein with RNA binding activity and a critical component of the viral replicase. *In silico* analysis suggests that NS5A encompasses three domains interconnected by two low-complexity sequences (LCSs). While domain I harbors two functional determinants, an N-terminal amphipathic helix important for membrane association, and a Zn-binding site essential for RNA replication, the structure and function of the C-terminal half of NS5A are still ill defined. In this study, we introduced a panel of 10 amino acid deletions covering the C-terminal half of NS5A. In the context of a highly efficient monocistronic replicon, deletions in LCS I and the N-terminal part of domain II, as well as in domain III, were tolerated with regard to RNA replication. When introduced into a bicistronic replicon, only deletions in LCS I and the N-terminal part of domain II were tolerated. In the context of the viral full-length genome, these mutations allowed residual virion morphogenesis. Based on these data, a functional monocistronic BVDV replicon coding for an NS5A variant with an insertion of the fluorescent protein mCherry was constructed. Live cell imaging demonstrated that a fraction of NS5A-mCherry localizes to the surface of lipid droplets. Taken together, this study provides novel insights into the functions of BVDV NS5A. Moreover, we established the first pestiviral replicon expressing fluorescent NS5A-mCherry to directly visualize functional viral replication complexes by live cell imaging.

The genus *Pestivirus* and the genera *Hepacivirus*, *Pegivirus*, and *Flavivirus* establish the family *Flaviviridae* (1). Pestiviruses, like classical swine fever virus (CSFV) and bovine viral diarrhea virus (BVDV), are important animal pathogens, causing major losses in stock farming. BVDV is an enveloped RNA virus with a 12.3-kb-long single-stranded, positive-sense RNA genome composed of a long open reading frame (ORF) flanked by 5′ and 3′ untranslated regions (UTRs) (2). An internal ribosomal entry site (IRES) located within the 5′ UTR promotes initiation of translation by cap-independent attachment of ribosomes to the initiation codon (3). The RNA genome is translated into a polyprotein, which is co- and posttranslationally cleaved by cellular and viral proteases to yield the mature viral structural and nonstructural (NS) proteins in the following order: NH_2-N^{pro}, C, E^{rns}, E1, E2, p7, NS2, NS3, NS4A, NS4B, NS5A, and NS5B-COOH (2). C, E^{rns}, E1, and E2 are the structural proteins (4). As in all RNA viruses, most of the BVDV nonstructural proteins serve central functions in viral RNA replication. The minimal part of the viral polyprotein required for autonomous RNA replication encompasses the NS3 to NS5B region (5). Moreover, for BVDV, the RNA sequence of the ORF immediately downstream of the IRES as well as the generation of the authentic N terminus of NS3 are critical for RNA replication (5–8). As a case in point, highly efficient RNA replication has been observed for a replicon with the genome structure of a natural defective interfering (DI) BVDV RNA encoding NH2-N^{pro}, NS3, NS4A, NS4B, NS5A, and NS5B-COOH (5, 9). In this polyprotein, the N terminus of NS3 is generated by the autoprotease N^{pro}, while the NS3 protease, in conjunction with its cofactor, NS4A, processes the remainder of the viral polyprotein (9, 10). Besides serine protease activity, the multifunctional NS3 protein also serves as a helicase/NTPase in viral RNA replication (11). NS5B is an RNA-dependent RNA polymerase (RdRp) which catalyzes viral RNA synthesis (12, 13). NS5A is a zinc metalloprotein that is phosphorylated by cellular kinases with an important but not completely clarified function in RNA replication (15, 16). To date, NS5A is the only replicase component that can be complemented in *trans* (17). The N terminus of BVDV NS5A has been demonstrated to form an in-plane amphipathic α-helix which anchors the protein to intracellular membranes, a feature that is believed to be essential for the formation of the functional replication complex (18). However, the structure and function of the downstream part of NS5A are still ill defined. Recently, CSFV NS5A has been shown to regulate CSFV viral RNA replication by either binding to the 3′ UTR of the viral RNA genome via its RNA binding activity or by modulating the RdRp activity of NS5B by direct protein-protein interactions (19, 20).

NS5A of the related hepatitis C virus (HCV) is also a zinc-binding phosphoprotein that is composed of 3 domains interspaced with two low-complexity sequences (LCS I and LCS II). An N-terminal amphipathic α-helix located in domain I anchors HCV NS5A to intracellular membranes (21–23). The ordered nature of the N-terminal domain I allowed the determination of its crystal structure, which suggested that it forms a dimer to which a single-strand RNA molecule can bind (23, 24). The RNA binding

Received 16 July 2013 **Accepted** 9 October 2013
Published ahead of print 16 October 2013
Address correspondence to Norbert Tautz, Tautz@vuz.uni-luebeck.de.

doi:10.1128/JVI.01957-13

capability of this protein was further corroborated by *in vitro* studies demonstrating that all three domains of HCV NS5A contribute to RNA binding (25, 26). In contrast to the rigid fold of domain I, domains II and III are believed to be intrinsically unstructured, and their interaction with cyclophilins is of importance for the viral life cycle (14, 27–32). Deletion studies revealed that large parts of domain II and domain III of HCV NS5A are not essential for RNA replication, and that most of domain III can be replaced by green fluorescent protein (GFP) without a significant effect on this process (33–35, 37). However, the C-terminal part of domain III encompasses a phosphorylation site that has been shown to represent a major determinant for HCV particle production (36). More recently, it has been shown that a fraction of HCV NS5A localizes at the surface of LDs (38–40). The localization of NS5A and other viral components, especially core protein, on LDs is a prerequisite for the production of infectious HCV particles (38, 41, 42). Studies concerning the subcellular sites of viral RNA replication and virion morphogenesis have been reinforced by live cell imaging employing HCV genomes which express a functional NS5A-GFP fusion protein (34, 43–46).

The aim of the present study was to gain insights into the functions of NS5A in the pestiviral life cycle. To this end, a reverse genetic analysis was conducted to determine the parts of BVDV NS5A downstream of the putative domain I which are required for pestiviral RNA replication and virion production, respectively. Taking advantage of a highly efficient BVDV replicon system, named DI-388, we tested 24 small deletions spanning the C-terminal half of the NS5A protein (residues 248 to 488) with regard to their influence on viral RNA replication. Analysis of this set of mutants in the BVDV DI-388 context identified two regions of 90 and 50 NS5A residues, respectively, which tolerate deletions. Viable NS5A deletion mutants were further surveyed for their effect on BVDV CP7 virus production.

These data were used to establish a functional BVDV replicon expressing fluorescent NS5A-mCherry, which allowed the detection of BVDV replication complexes in living cells for the first time. Live cell imaging revealed that, analogous to NS5A of HCV, a fraction of BVDV NS5A localizes to LDs. Taken together, this study revealed critical functions of the C-terminal region of BVDV NS5A in the pestiviral life cycle.

MATERIALS AND METHODS

Cells and viruses. Madin-Darby bovine kidney (MDBK) cells were obtained from the American Type Culture Collection (Rockville, MD) and grown in Dulbecco's minimum essential medium (DMEM) with 10% horse serum (PAA, Cölbe, Germany), nonessential amino acids, 100 U/ml penicillin, and 100 μg/ml streptomycin. Huh7-T7 cells, a Huh7 cell line stably expressing T7 RNA polymerase (47) (a kind gift of Stan Lemon; UNC, Chapel Hill, NC), were grown in DMEM with 10% fetal calf serum (FCS gold; PAA), 100 U/ml penicillin, 100 μg/ml streptomycin, and 1 mg/ml G418. All cells were grown at 37°C and 5% CO_2.

Vaccinia virus modified virus Ankara (MVA)-T7pol (48) was generously provided by G. Sutter (LMU, Munich, Germany). The cytopathogenic BVDV-1 strain CP7 was generated from the authentic full-length infectious BVDV cDNA clone pCP7-388, which has been described previously (49).

Antibodies. For immunological detection of BVDV proteins, the following mouse monoclonal antibodies (MAbs) were used: NS3, 8.12.7 (50); NS4A, GH4A1 ([4B7]) (51); NS5A, GLBVD5A1 (11C) (unpublished); and NS5B, GLBVD5B1 (9A) (unpublished). Goat anti-mouse IgG antibody coupled to horseradish peroxidase (α-mouse-HRP) was used as the secondary antibody (Dianova, Hamburg, Germany) for Western blot analysis. Goat anti-mouse IgG secondary antibody conjugated with Cy3 (Dianova, Hamburg, Germany), Alexa Fluor 647, or Alexa Fluor 488 (Invitrogen, Molecular Probes, Darmstadt, Germany) was used for indirect immunofluorescence assays.

Plasmid constructs. Plasmids were constructed by standard methods. All mutations were introduced either by standard PCR or by the QuikChange *in vitro* mutagenesis system by following the manufacturer's standard protocols (Stratagene, Heidelberg, Germany). The resulting PCR or QuikChange products were verified by sequencing, and the integrity of all final plasmid constructs was analyzed by restriction enzyme digestion and DNA sequencing. The plasmid pCP7-388 encodes the full-length BVDV CP7 cDNA genome (49). The replicon encoded by plasmid pDI-388 is based on the natural BVDV isolate DI9 and contains the 5′ and 3′ UTRs flanking the genes encoding N^{pro} followed by NS3 to NS5B (5, 9, 52). Upstream of the viral cDNA, an SP6 RNA polymerase promoter was integrated in such a way that the start site of the RNA transcript is the first nucleotide of the BVDV cDNA. A singular SmaI site allows linearization of the plasmids at the 3′ end of the cDNA, leading to molecules with three terminal C residues. In the pT7-DI-388 plasmid the SP6 polymerase promoter of pDI-388 was replaced by the T7 promoter sequence upstream of the BVDV 5′ UTR to allow the transcription of the BVDV DI-388 cDNA by T7 RNA polymerase. In order to establish an assay that allows quantitative analysis of the viral replication potential of the mutant RNA replicons in MDBK cells, bicistronic BVDV replicons (pBici-388 RLuc NS3-3′) expressing a *Renilla* luciferase (RLuc) reporter gene downstream of the N^{pro} coding sequence in the first open reading frame were generated. The RLuc gene in pBici-388 RLuc NS3-3′ was derived from pF/R-wt (53), kindly provided by Ann Palmenberg (Madison, WI), by PCR amplification with primers BssHII RLuc sense (5′-GCGCGCATACCATGGCTTC CAAGGTGTACGACCCC-3′) and FseI RLuc antisense (5′-GGCCGGCC ATTACTGCTCGTTCTTCAGCACGCGC-3′) and subsequently fused in frame via BssHII and FseI to the 3′ end of the N^{pro} coding sequence. Downstream of the stop codon of the RLuc gene, a PvuII/SacI fragment (nucleotides 3690 to 590) of pCITE2a (Novagen, Madison, WI) was integrated. This fragment encompasses the IRES of encephalomyocarditis virus (EMCV). The cDNA in the resulting plasmid, pBici-388 RLuc NS3-3′, which served as the basis for all further bicistronic constructs, encompasses the following sequences downstream of the SP6 RNA polymerase promoter: the 5′ UTR, the N^{pro} coding sequence, RLuc gene sequence, and the EMCV IRES. The ORF downstream of the EMCV IRES encompasses the methionine start codon, followed by the sequence for the CP7 polyprotein starting with the NS3 glycine^{1590} and followed by the 3′ UTR of the CP7 genome. A singular SmaI site allows linearization of the plasmids at the 3′ end of the cDNA.

To construct the bicistronic Bici-388 RLuc NS2-3′ replicon, a region encompassing BVDV CP7 genomic sequence 3809 to 5359, including the entire NS2 and the N terminus of NS3, was amplified using the primers BVDV NS2 BsmBI se (5′-CGTCTCCCATGGAACCAGGTGCCCAGGG GTACCTAGAGCAGGTAGACC-3′) and BVDV NS3 AgeI ase (5′-ACCG GTTTCCAATCCCCTCCTTACCTTTAGTAGTGCTG-3′), where the underlined sequences correspond to the BsmBI and AgeI restriction sites. Cleavage with BsmBI restriction enzyme would generate an NcoI-compatible overhang at the 5′ end of the fragment, thereby allowing the insertion of the NS2 coding sequence directly downstream of the EMCV IRES into pBici-388 RLuc NS3-3′. The PCR product was cloned into pGEM-T (Promega, Madison, WI). The obtained pGEM-T NS2-3AgeI plasmid was subsequently cleaved with BsmBI and AgeI, and the fragment was cloned into pBici-388 RLuc NS3-3′ treated with NcoI and AgeI, resulting in pBici-388 Rluc NS2-3′.

All NS5A deletions were generated via QuikChange mutagenesis with the subclone vector pKS(+)Sal-NS5A-Cla as the template, which contained the SalI-ClaI fragment derived from the pCP7-388 plasmid encompassing the NS5A coding sequence and surrounding regions. To construct this plasmid, pCP7-388 was digested with SalI and ClaI (NEB, Frankfurt/Main, Germany), and the NS5A-encoding fragment was gel purified and

ligated into pBluescript II KS(+) (Agilent Technologies, Waldbronn, Germany) cleaved with the same enzymes. All NS5A deletion mutations derived from the pKS(+)Sal-NS5A-Cla plasmids were ligated into pDI-388, pBici-388, pT7-DI-388, and pCP7-388 plasmids via SalI and ClaI restriction sites to obtain either the final monocistronic or bicistronic replicon plasmids or the pCP7-388 full-length cDNA constructs. A list of the sequences of the primers used for QuikChange mutagenesis is available upon request.

The NS5A deletion 258-337 was generated as follows. The region encoding BVDV sequence from positions 7766 to 9248 (numbering refers to the BVDV CP7 genome sequence and includes the C-terminal half of the NS4B coding sequence and the first 257 amino acids [aa] of NS5A) was amplified with the primers BVDV Sal-NS5A-AS258 forward (fwd) (5′-GTCGACCTGGTTGTTTATTATGT GATCAATAAGCCCTCC-3′) and BVDV Sal-NS5A-AS258 reverse (rev) (5′-GCTAGC**AGATCC**GGTGAC CACTCTCTCTCCTAGTACTGGTTTTATAGTCCC-3′). Underlined sequences in the fwd and rev primers indicate the SalI and NheI restriction sites, respectively. The boldface sequence in the rev primer depicts the sequence for glycine and serine amino acid codons which were introduced as a linker sequence following NS5A amino acid 257. To amplify BVDV region 9488-11099 (numbering refers to the BVDV CP7 genome and covers the C-terminal NS5A region starting with amino acid 338 and the first 378 aa of the NS5B coding region), the primers BVDV AS337-NS5A-Cla fwd (5′-GCTAGC**GGTTCA**AGGCCCTTTGTTCTAGTCCTGGGCT CAAAAAATTCTATG-3′) and BVDV AS337-NS5A-Cla rev (5′-TATCG ATGAATTTGTGCCACTCTTTCCTGTAGTAATATTTTTG-3′) were used. Underlined sequences in the fwd primer and in the rev primer indicate the NheI and ClaI restriction sites, respectively. The boldface sequence in the fwd primer depicts the sequence for additional glycine and serine amino acid codons, which were introduced as a linker sequence preceding NS5A amino acid 338. The PCR products were cloned into pGEM-T vector (Promega, Madison, WI), resulting in pGEM-T BVDV Sal-NS5A-AS258 and pGEM-T BVDV AS337-NS5A-Cla, respectively. For the generation of pDI-388 NS5A Δ258-337, a three-fragment ligation was performed. The fragments were (i) fragment Sal-NS5A-AS258, obtained from pGEM-T BVDV Sal-NS5A-AS258 via SalI and NheI, (ii) fragment AS337-NS5A-Cla, generated by NheI and ClaI restriction, and (iii) the vector fragment (originating from pBVDV DI-388 cleaved with SalI and ClaI). For the generation of pBVDV Bici-388 Δ258-337, pBVDV Bici-388 was cleaved with SalI and ClaI and used for the ligation reaction. The resulting plasmids encode an NS5A variant with a deletion spanning aa 258 to 337; NS5A aa 257 and 338 are connected via a Gly-Ser-Ala-Ser-Gly-Ser linker.

The mCherry coding sequence was amplified from pcDNAmCherry using the primers Mlu-mCherry sense (5′-ACGCGTTTGAGCAAGGGC GAGGAGGATAAC-3′; underlined sequence indicates the MluI restriction site) and Asc-mCherry antisense (5′-GGCGCGCCCTTGTACAGCT CGTCGTCCAT-3′; the underlined sequence indicates the AscI restriction site), and the PCR product was ligated into the pGEM-T vector (Promega, Mannheim, Germany), resulting in pGEM-T-Mlu-mCherry-Asc. The plasmid pKS(+)Sal-NS5A-mCherry-Cla is based upon pKS(+)Sal-NS5A-Cla and was generated as follows. First, MluI and AscI sites were introduced into pKS(+)Sal-NS5A-Cla via two consecutive QuikChange *in vitro* mutagenesis reactions using primers NS5A Mlu QC sense (5′-GTTGGTAGGGCAGCCTTAATGACGCGTGGTACTACACCC GTAGTCG-3′) and NS5A Asc QC sense (5′-CGACAGGTACTACACCCGT AGTCGGCGCGCCAGAGCCCAATGCTGATGGTCC-3′), where the underlined sequence represents the MluI and AscI restriction sites, resulting in pKS(+)Sal-Mlu/NS5A/Asc-Cla. Second, the mCherry coding sequence was excised from pGEM-T-Mlu-mCherry-Asc with MluI and AscI restriction enzymes and was introduced into pKS(+)Sal-Mlu/NS5A/Asc-Cla via the same sites in frame into the NS5A coding sequence downstream of codon 288, replacing NS5A codons 289 to 297 and resulting in pKS(+)Sal-NS5A-mCherry-Cla. To generate the plasmid pT7-DI-388mCherry, pKS(+)Sal-NS5A-mCherry-Cla was digested with SalI and ClaI restriction enzymes, and the fragment containing the NS5A-mCherry coding sequence was subsequently ligated into pT7-DI-388 cut with the same enzymes.

To construct pNS5A-mCherry, the NS5A-mCherry coding sequence was amplified from pKS(+)Sal-NS5A-mCherry-Cla with primers NS5A-fwd (5′-GGTACCATGTCTGGGAAT TATGTCCTGGATTTG-3′) and NS5A-stop-rev (5′-GGATCCTTACAGCTTCATGGTATA GGTTCTTG C-3′), where the underlined sequences represent KpnI and BamHI restriction sites. The PCR product was digested with KpnI and BamHI, gel purified, and ligated into peYFP-N1 (Clontech, Palo Alto, CA) cleaved with the same restriction enzymes; the stop codon downstream of mCherry prevents yellow fluorescent protein (YFP) expression. peGFP-N1-Perilipin was obtained from Hans Heid (German Cancer Research Center, Heidelberg, Germany). The plasmid pmCherry-KDEL was kindly provided by Gia Voeltz (University of Colorado).

***In vitro* transcription and electroporation.** Plasmid DNA (10 μg) was linearized with SmaI (NEB, Frankfurt/Main, Germany) at the 3′ end of the respective cDNA and subsequently purified by phenol-chloroform extraction and ethanol precipitation. RNA transcripts were synthesized with the MAXIscript SP6 and T7 kits (Ambion, Austin, TX), followed by DNase I digestion according to the protocol of the manufacturer. The yield of RNA was determined by quantification with the Quant-iT RNA assay kit and the Qubit fluorometer (Invitrogen, Karlsruhe, Germany). The quality of RNA was further confirmed by agarose gel electrophoresis.

For RNA electroporation, confluent MDBK cells from a 10-cm dish were trypsinized, washed, resuspended in 0.4 ml of 1× phosphate-buffered saline (PBS; Accugene, Lonza, Hessisch Oldendorf, Germany), and mixed with 1 μg of *in vitro*-transcribed RNA immediately before the pulsing step (2-mm gap cuvette, 950 μF, 180 V). The electroporation was performed with a Gene Pulser Xcell (Bio-Rad, Munich, Germany). The electroporated cells were resuspended in 0.6 ml of medium containing 10% horse serum, and this cell suspension was then seeded immediately postelectroporation (pe). At the indicated time points, cells were processed for Renilla luciferase assay or immunofluorescence assay, or supernatants were used for determination of viral yields after electroporation. For live cell imaging, RNA transcripts (5 μg) were electroporated alone or together with peGFP-N1-Perilipin (5 μg) into MDBK cells (2-mm gap cuvette, 950 μF, 180 V). pNS5A-mCherry (5 μg) was always electroporated individually. Fluorescence was detected at 18 h pe for the DI-388 wild type (WT), at 24 h pe for pNS5A-mCherry, and at 48 h pe for DI-388mCherry.

Isolation and quantification of intracellular and released BVDV RNA. To quantify intracellular BVDV RNA, total cellular RNA was prepared from 1×10^6 electroporated MDBK cells at 30 and 48 h pe using the RNeasy mini kit (Qiagen, Hilden, Germany) according to the instructions of the manufacturer and dissolved in 30 μl RNase-free double-distilled H_2O (ddH_2O). For the quantification of BVDV genome release, total RNA was isolated from 140 μl clarified cell culture supernatant of a total of 2 ml supernatant using a QIAamp viral RNA mini kit (Qiagen, Hilden, Germany) by following the instructions of the manufacturer and diluted in 60 μl RNase-free ddH_2O. cDNA synthesis was performed at 53°C using SuperScript III reverse transcriptase (Invitrogen, Carlsbad, CA) with a 1/3 volume of extracted total intracellular or 1/6 volume of the extracted total released RNA. Quantitative reverse transcription-PCRs (qRT-PCRs) were performed using a Maxima probe/ROX qPCR master mix (Fisher Scientific, Schwerte, Germany) and run with an iCycler iQ real-time PCR detection system (Bio-Rad, Munich, Germany) on the absolute quantification setting according to the manufacturer's instructions. To quantify viral genomic BVDV RNA in electroporated MDBK cells, the BVDV-1-specific probe pvtaq01 (6-carboxyfluorescein-ACAGTCTGATAGGATG CTGCAGAGGCCC-6-carboxytetramethylrhodamine) and the primer pair pv02 (GTGGACGAGGGCATGCC)-pv03R (TCCATGTGCCATGT ACAGCAG) were used (54).

Nucleotide sequencing. A DNA sequencing service from Qiagen or LGC Sequencing Services (Berlin, Germany) was used. Sequences were further analyzed by using Vector NTI software (Invitrogen, Karlsruhe, Germany).

Vaccinia virus infection, DNA transfection, and transient protein expression. A total of 2×10^6 Huh7-T7 cells per 3.5-cm tissue culture dish were infected with MVA-T7pol at a multiplicity of infection (MOI) of 2 in 1 ml culture medium lacking serum and antibiotics for 1 h at 37°C. For transfection of pT7-DI-388 plasmid DNA (4 μg), Superfect reagent was applied (Qiagen, Hilden, Germany) according to the manufacturer's standard protocol.

SDS-PAGE and immunoblotting. Proteins were separated in polyacrylamide-Tricine gels (8, 10, or 12% polyacrylamide) (55). After SDS-PAGE, proteins were transferred onto nitrocellulose membrane (Pall, Pensacola, FL). The membrane was blocked with 5% (wt/vol) dried skim milk in phosphate-buffered saline with 0.05% (vol/vol) Tween 20 (Invitrogen, Karlsruhe, Germany). For antigen detection, peroxidase-coupled species-specific secondary antibodies and Western Lightning chemiluminescence reagent plus (PerkinElmer, Boston, MA) were applied.

BVDV infection and virus titration. Supernatants of electroporated cells were filtered using a 0.2-μm cellulose filter (Sartorius, Göttingen, Germany). Infection with BVDV was carried out as described previously for 1 h at 37°C (56). Endpoint titration was performed in three replicates on MDBK cells. Virus detection occurred after 72 h by indirect immunofluorescence analysis (IF) using MAb 8.12.7 directed against NS3 of BVDV and a secondary cyanogen-3-labeled antibody as described previously (56).

Immunofluorescence assay and confocal microscopy. MDBK cells were seeded into 6-well plates containing glass coverslips (diameter, 25 mm). They were infected with recombinant BVDV-1 CP7 derived from pCP7-388 at a multiplicity of infection (MOI) of 2. Forty-eight h postinfection (pi), cells were fixed by 4% paraformaldehyde for 20 min at 4°C. Afterwards, cells were permeabilized by 0.5% (wt/vol) N-octylglucopyranoside in PBS for 7 min at room temperature. The mouse anti-BVDV NS5A (diluted 1:3 in PBS) or anti-BVDV NS3 (diluted 1:40 in 1× PBS, 0.05% Tween 20) antibody served as the primary antibody. Goat anti-mouse IgG conjugated with Cy3 was used at 1:1,000 and served as the secondary antibody. Images were obtained with a Zeiss Axio Observer.Z1 fluorescence microscope (Zeiss, Göttingen, Germany). Live cell imaging was performed on cells electroporated with BVDV DI-388mCherry RNA or pNS5A-mCherry DNA without fixation and immunostaining. Lipid droplets were stained with Bodipy 493/503 (4,4-difluoro-1,3,5,7,8-pentamethyl-4-bora-3a,4a-diaza-s-indacene; Invitrogen Molecular Probes). Imaging of fixed samples and live cell imaging was performed using a Nikon Ti Eclipse-based spinning disk confocal microscope as described in detail by Willett et al. (57). Line plots were generated using the RGB profiler plug-in of Image J (58).

Protein secondary structure prediction. The program SEG was used to identify potential LCSs within NS5A (59). Secondary structure predictions were performed using the JPRED server (60).

RESULTS

Domain I of BVDV NS5A has been shown to encompass an amphipathic helix serving as a membrane anchor and a Zn-binding site, which is essential for viral RNA replication (16). For the remainder of this protein, neither the domain structure nor the functional relevance for RNA replication and virion morphogenesis has been determined in detail.

The NS5A proteins of BVDV and HCV share a low sequence identity of about 15% (data not shown). Therefore, it was not possible to delineate the domain structure of BVDV NS5A by a sequence alignment using HCV NS5A as the template. Consequently, we performed an *in silico* analysis of the BVDV NS5A protein sequence by applying several secondary structure prediction programs. With the aim to develop a domain organization model of BVDV NS5A, we used the program SEG, an algorithm that predicts repetitive low-complexity sequences in proteins, to identify the interdomain boundaries connecting the putative domains of BVDV NS5A. With this program, two potential LCSs were identified in NS5A, designated LCS I (residues 249 to 282) and LCS II (residues 428 to 437) (Fig. 1B). According to this prediction, BVDV NS5A is composed of three domains (domains I, II, and III) (Fig. 1B) interconnected by LCS I and II, comparable to HCV NS5A.

To study the functional relevance of domains II and III of BVDV NS5A, 24 colinear deletion mutants were generated such that they spanned amino acids 248 to 488 of the NS5A protein. Domain I of NS5A was not included in this study, since it was previously shown to be essential for RNA replication (16). Amino acids 489 to 496 were not analyzed in order to avoid interference of the polyprotein processing at the NS5A/NS5B junction. To test the effect of these mutations on RNA replication, the individual deletions were introduced into the BVDV replicon DI-388 encoding N^{pro} followed by NS3 to NS5B (Fig. 1A). This replicon is based on the natural BVDV isolate DI9 and replicates with high efficiency (5, 61). The different DI-388 RNAs were electroporated into MDBK cells, and detection of NS3 via an immunofluorescence assay (IF) was used to monitor viral RNA replication at 20 h postelectroporation (pe). Wild-type (WT) DI-388 and a derivative with an inactivating mutation in the RdRp domain of NS5B (DI-388/GAA) were used as positive and negative controls, respectively. The WT replicon replicated efficiently, as indicated by the induction of a severe cytopathic effect (CPE) beginning at 16 h pe (Fig. 2 and data not shown), while no RNA replication was detectable in cells electroporated with the DI-388/GAA replicon RNA, as expected (Fig. 2, compare WT and GAA). In the context of this system, replicon RNAs with 10-aa deletions in the NS5A regions spanning aa 248 to 337 as well as aa 438 to 488 were capable of RNA replication, as visualized by the NS3-specific IF assay at 20 h pe, while deletions of aa 338 to 437 prevented detectable RNA replication (Fig. 2). Interestingly, the viable NS5A deletions did affect viral RNA replication to different degrees; while deletions spanning aa 258 to 337 allowed for robust RNA replication, the replicon RNAs with NS5A deletions of aa 248 to 257 and 438 to 488 replicated less efficiently, reflected by lower fluorescence intensities in the IF assay.

In order to estimate the relative RNA replication capacities of the individual NS5A deletion variants quantitatively, each of the mutations was introduced into the bicistronic replicon Bici-388 RLuc NS3-3′ expressing RLuc downstream of N^{pro}. In this replicon, N^{pro} and RLuc are translated under the control of the BVDV IRES, while translation of the viral nonstructural proteins NS3 to NS5B is initiated from an EMCV IRES located downstream of the stop codon of the RLuc gene (Fig. 1A). The individual Bici-388 RLuc NS3-3′ replicon RNAs were electroporated into MDBK cells. Cell extracts were analyzed for RLuc activity at 2, 24, and 30 h pe (Fig. 3) and expression of NS3 by IF at 48 h pe (data not shown). The 2-h value was representative of both RNA electroporation efficiency and input translation of the individual bicistronic replicon RNAs. The RLuc activity in cells was about a factor of 100 above that of the mock control at 2 h pe. In lysates of cells electroporated with the wild-type replicon, the RLuc activity was similar to that obtained from cells harboring the replication-deficient derivative Bici-388 RLuc NS3-3′ GAA RNA (Fig. 3A). This observation confirmed that in the first 2 h after electroporation, RLuc activity is exclusively produced by translation of the electroporated input bicistronic replicon RNAs. The RLuc activities obtained at 2 h pe confirmed that comparable electroporation efficiencies were achieved for all Bici-388 RLuc NS3-3′ derivatives. At

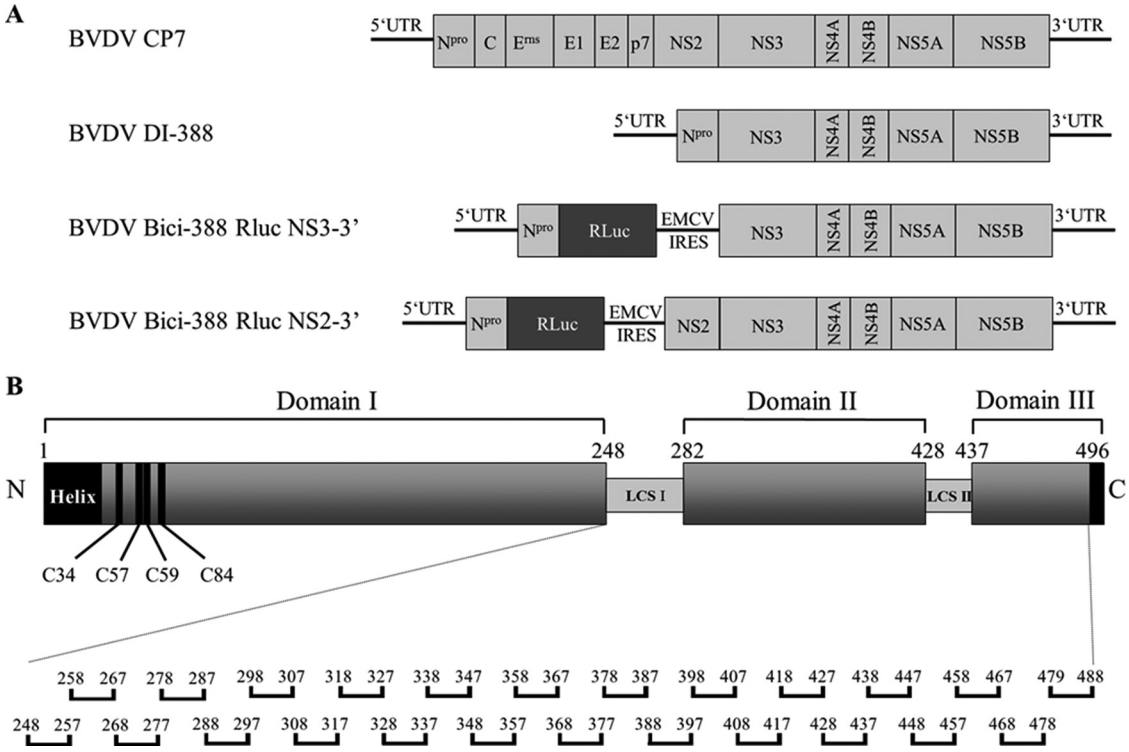

FIG 1 (A) Schematic organization of BVDV RNAs used in this study. BVDV CP7 represents the full-length genomic RNA of BVDV-1 strain CP7. BVDV DI-388 is a monocistronic replicon RNA with the N^{pro} coding sequence directly fused to NS3 to generate the authentic N terminus of NS3. BVDV Bici-388 RLuc NS3-3′ is a bicistronic RNA replicon, with ORF1 comprising the N^{pro} coding sequence fused to the Renilla luciferase sequence (black box) and the BVDV proteins NS3 to NS5B encoded by ORF2 downstream of the EMCV IRES. In BVDV Bici-388 RLuc NS2-3′, the BVDV proteins NS2 to NS5B are encoded by ORF2 downstream of the EMCV IRES. The 5′ and 3′ UTRs are shown as black lines, and the polyprotein cleavage products are indicated by light gray boxes. (B) Schematic representation of the BVDV NS5A protein. BVDV NS5A has been predicted to be composed of three putative domains (dark gray boxes; domains I, II, and III) connected by low complexity sequences (small light gray boxes; marked LCS I and II). The amino-terminal amphipathic helix membrane anchor is shown as a black box (Helix). The black box at the C terminus of NS5A represents amino acid residues 489 to 496, which were not included in the deletion mutagenesis. The zinc-binding site with the four conserved cysteine residues (black bars; C34, C57, C59 and C84) is indicated in domain I. The amino (N) and carboxyl (C) termini of NS5A are marked. All numbers refer to the amino acid numbering of BVDV CP7 NS5A, with the amino terminus of the mature protein set as amino acid 1. The approximate positions of deletions introduced into BVDV NS5A are shown as black brackets below the domain organization representation. Numbers above each bracket define the amino acids deleted. The dotted lines mark the N- and C-terminal borders of the deletion mutagenesis set.

24 h pe, the RLuc activity derived from cells containing Bici-388 RLuc NS3-3′ WT RNA was about 100-fold higher than the RLuc activity in cells electroporated with the nonreplicating replicon Bici-388 RLuc NS3-3′ GAA RNA, indicating active RNA replication. At 24 h pe, elevated RLuc activity compared to that of the Bici-388 RLuc NS3-3′ GAA RNA control was observed only in lysates of cells electroporated with replicon RNAs harboring deletions in the NS5A region spanning amino acids 258 to 337. For all of these replicon RNAs, a further increase in the RLuc activity was detectable at 30 h pe, confirming the replication competence of these mutants. Compared to the 24-h value, a decrease in the RLuc activity was observed in cells electroporated with the Bici-388 RLuc NS3-3′ WT RNA, implying the induction of a cytopathic effect (compare Fig. 3B and C). For cells containing Bici-388 RLuc NS3-3′ NS5AΔ248-257, the initial decrease of RLuc activity at 24 h pe compared to the 2-h value was followed by a significant increase between 24 and 30 h pe. In contrast, in lysates of cells electroporated with the bicistronic replicons harboring deletions of NS5A amino acids 338 to 347 to amino acids 479 to 488, no increase in RLuc activity was detectable at 24 or 30 h pe compared to the respective 2-h values, indicating that these RNAs are replication deficient (Fig. 3).

Interestingly, some NS5A deletions (438-447, 448-457, 458-467, 468-478, and 479-488), while being tolerated in the context of the efficient monocistronic DI-388 replicon RNA, did not allow for viral replication in the context of the less efficient bicistronic Bici-388 RLuc NS3-3′ replicon. In agreement with the results obtained by the RLuc assay, the IF analysis of cells electroporated with Bici-388 RLuc NS3-3′ NS5AΔ248-257 also showed only weak NS3 signals, while a robust NS3 expression was observed for Bici-388 RLuc NS3-3′ derivatives with deletions in the NS5A region of aa 258 to 337 (data not shown). Again, in agreement with the RLuc data obtained, all bicistronic replicons with NS5A deletions between aa 338 and 488 failed to produce any IF-detectable NS3 expression at 48 h pe (data not shown), further supporting the observation that these bicistronic replicon RNAs are not capable of replication. This demonstrates that the RLuc- and IF-based assays delivered congruent results for the bicistronic NS5A mutants. To address the question of whether the deletions tolerated individually can be combined to produce a minimal NS5A protein that remains viable, we introduced a larger deletion spanning amino acids 258 to 337 into the NS5A protein and tested if this NS5A protein is able to support viral RNA replication. A mono- as well as a bicistronic replicon harboring the 258-337 deletion failed

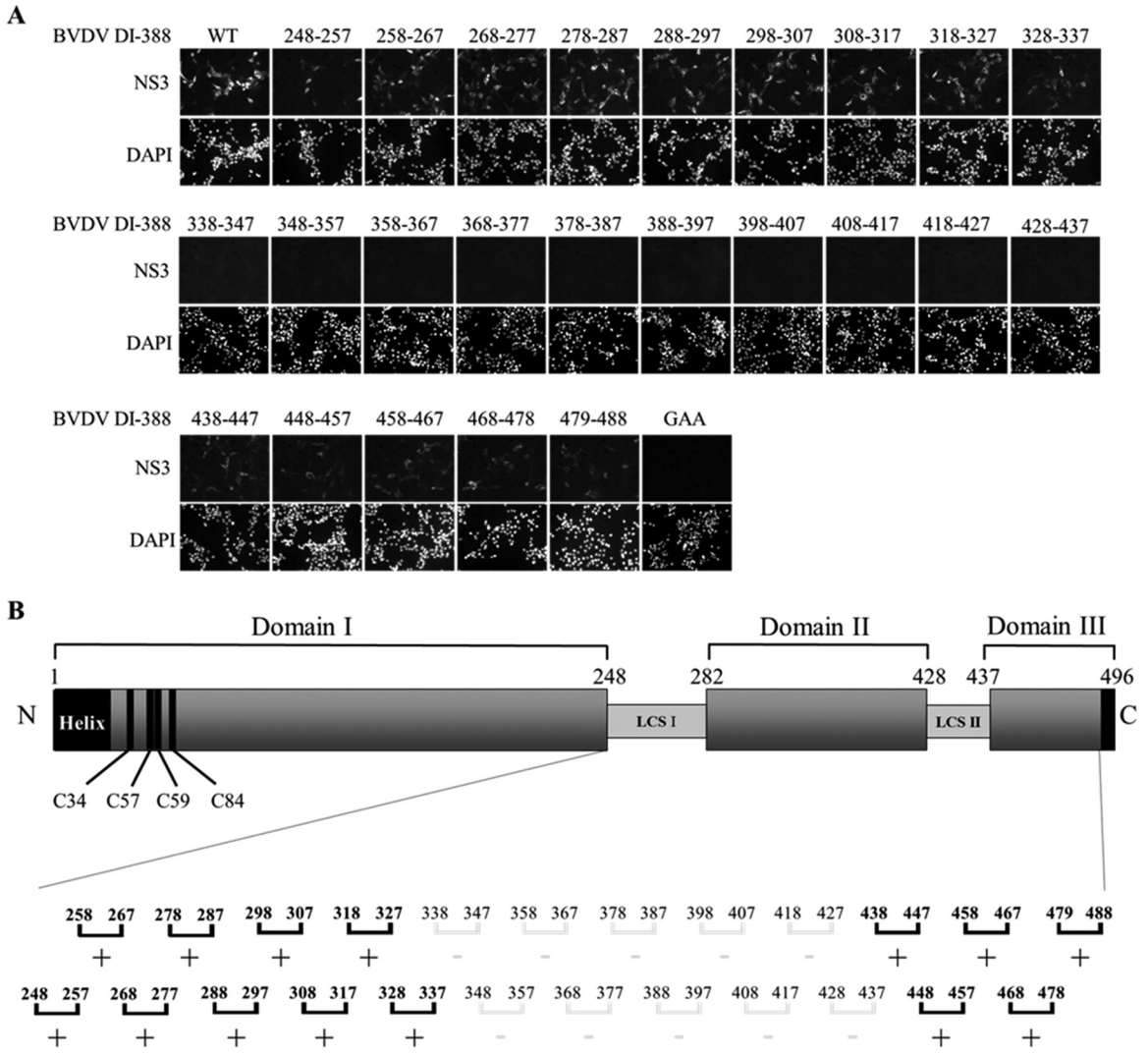

FIG 2 Analysis of replication phenotypes of BVDV DI-388 replicon RNAs bearing deletions in NS5A. (A) BVDV DI-388 replicon RNAs were electroporated into MDBK cells as described in Materials and Methods. At 20 h pe, cells were fixed and probed with an NS3-specific antibody to assess RNA replication (top rows, NS3) by indirect immunofluorescence using a Cy3-labeled secondary antibody. The nuclei were visualized by DAPI staining (bottom rows, DAPI). The wild-type (WT), the replication-deficient GAA, and the NS5A mutant DI-388 RNAs indicated above the individual pictures were analyzed. The non-replication-competent DI-388 GAA RNA harbors a lethal mutation in the NS5B RNA-dependent RNA polymerase and served as a negative control. (B) Deletions indicated with solid black brackets (+) allow for BVDV RNA replication in the context of the DI-388 replicon. Deletions labeled with light gray brackets (−) are not viable in the BVDV replicon system. The designations for NS5A are described in the legend to Fig. 1B. The results are representative of three independent RNA transcription/electroporation experiments.

to replicate detectably when electroporated into MDBK cells even at 48 h pe, while replicons with deletions of either aa 258 to 267 or 328 to 337 did replicate after 24 and 48 h pe (data not shown).

NS5A deletion mutants that inhibit RNA replication do not disrupt polyprotein processing. Most of the NS5A deletion mutations tested were deleterious with regard to viral RNA replication. One explanation, besides a critical effect of the deletions on NS5A function in the RNA replication complex, could be aberrant polyprotein processing or reduced NS5A stability due to an altered NS5A protein structure. To clarify these aspects, the entire pDI-388 series of cDNA constructs was cloned under the control of a T7-RNA polymerase promoter to allow expression of the viral polyproteins independently of their ability to support RNA replication. To this end, Huh7-T7 cells were first infected by vaccinia virus MVA T7-pol, subsequently transfected with the individual pT7-DI-388 plasmids, and then incubated for 18 h at 37°C to express the viral replicase proteins in a replication-independent manner. Cell lysates were analyzed by Western blotting by applying MAbs specific for NS3, NS4A, NS5A, and NS5B. Lysates of cells transfected with pT7-DI-388/WT and pT7-DI-388/GAA served as controls. All NS5A deletion mutants showed polyprotein processing unaltered from that of wild-type or GAA controls (Fig. 4A). Some of the mutant NS5A proteins exhibited slightly lower expression levels than the WT NS5A (Fig. 4A, compare WT to 338-347 or 358-367). This observation suggests that these deletions affect the stability of the protein; however, a pulse-chase analysis would be required to confirm this hypothesis.

Taken together, these data demonstrate that the inability of the NS5A mutants with deletions of regions 338-347 to 479-488 to

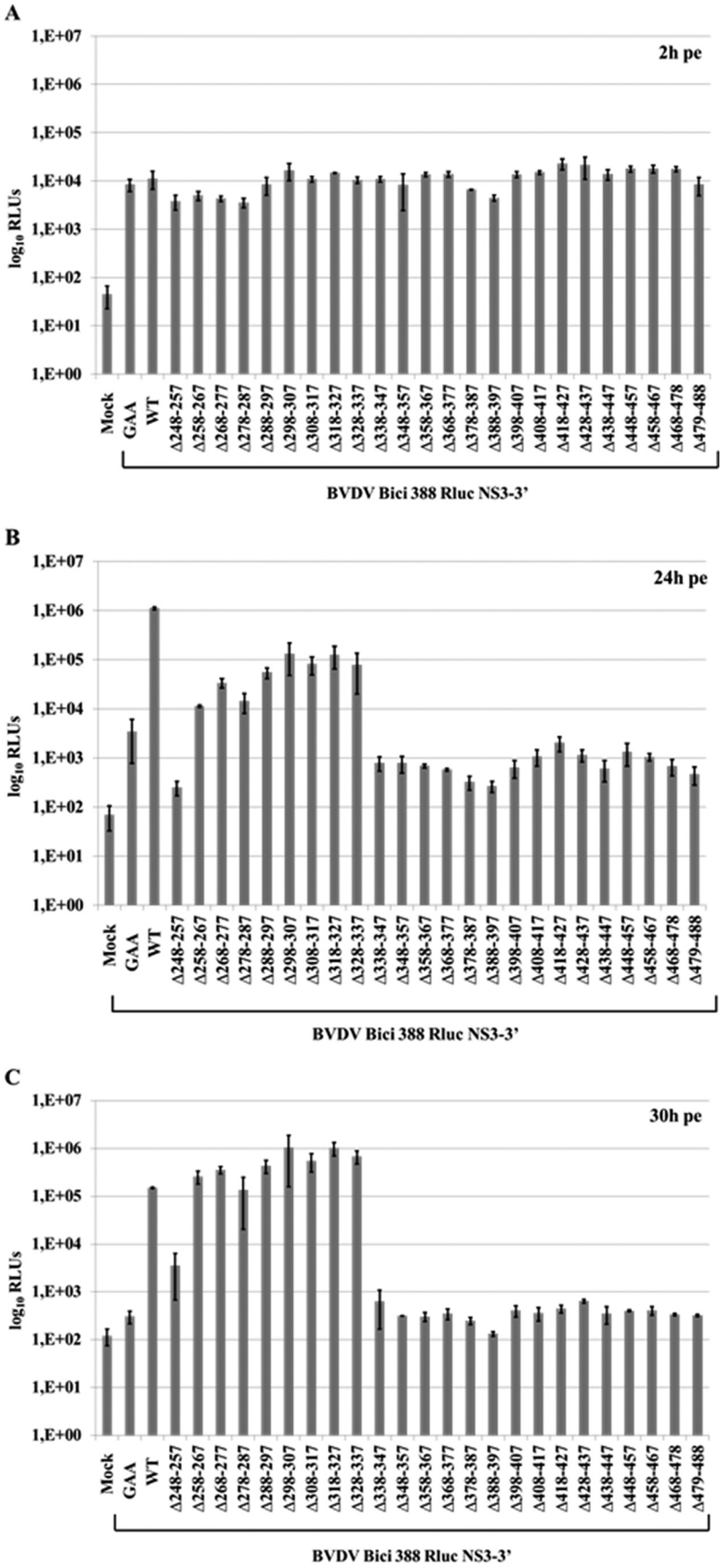

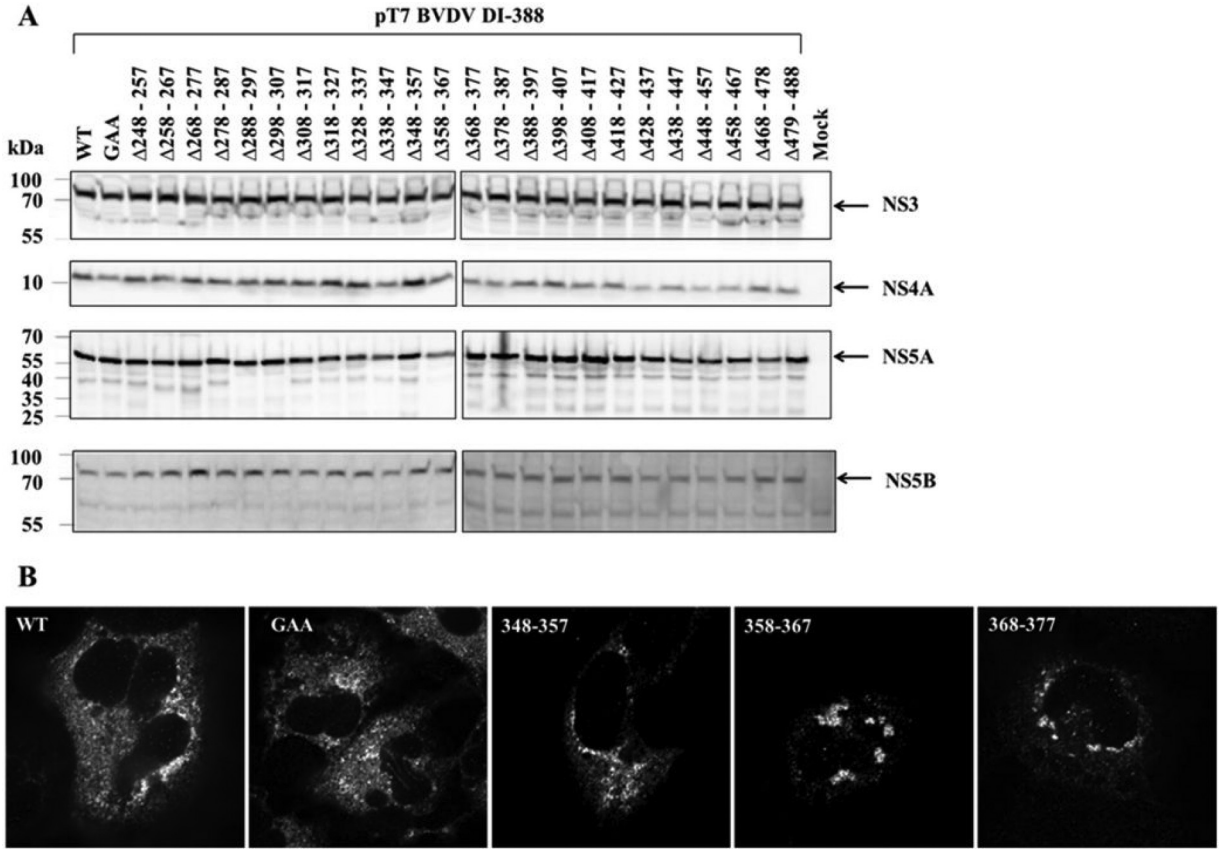

FIG 4 Effects of NS5A deletions on intracellular protein expression, localization, and proteolytic processing. The NS3-5B polyprotein was expressed from pT7-DI-388/WT or derivatives in Huh7-T7 cells using an MVA-T7 expression system. Huh7-T7 cells infected with MVA-T7pol vaccinia virus for 1 h were transfected with the DNAs indicated. The cells were incubated for 18 h at 37°C and subsequently processed for Western blot analysis (A) or immunofluorescence (B). (A) The cell lysates were separated by SDS-PAGE and analyzed by Western blotting using specific antibodies directed against NS3, NS4A, NS5A, and NS5B, respectively. WT, pT7 BVDV DI-388/WT; GAA, pT7 BVDV DI-388/GAA; Δ248-257 through Δ479-488, pT7 BVDV DI-388/NS5A mutants. Mock refers to cell lysates infected with MVA-T7 and transfected with empty pCITE2A vector control. The positions of the NS proteins are indicated on the right. The molecular mass standard is given on the left. (B) For immunofluorescence, cells were stained with the anti-NS5A monoclonal antibody. Images were taken by confocal microscopy.

support detectable viral RNA replication in the context of bicistronic replicons did not correlate with an obvious defect in polyprotein processing. Another reason for the observed replication phenotypes of the NS5A mutants could be aberrant intracellular localization/folding. To address this possibility, we used the same Huh7-T7 system and observed that membrane association of NS5A mutants was retained. In contrast to the wild type, we observed for the replication-deficient NS5A mutants a clustering of this protein to different degrees (Fig. 4B, compare 358-367 and 348-357 to the wild type, and data not shown), suggesting aberrant protein folding.

Effect of the NS5A deletions on virion morphogenesis. The results obtained so far indicated that NS5A mutants with deletions located within amino acids 248 to 337 of NS5A support viral RNA replication in the context of bicistronic Bici-388 RLuc NS3-3′ replicon RNAs, albeit with various efficiencies. We next investigated if these deletions in NS5A were tolerated in the context of the full-length infectious cDNA clone pCP7-388 with regard to genome replication and the production of infectious virus particles. Consequently, the nine individual NS5A deletions (248-257 to 328-337) were introduced into the full-length infectious pCP7-388 cDNA. The transcripts of pCP7-388/WT and its replication-deficient derivative pCP7-388/GAA served as controls. The *in vitro*-transcribed RNAs were electroporated into MDBK cells and assayed at 48 h pe for viral RNA replication by NS3-specific IF. In MDBK cells electroporated with genome-length transcripts coding for NS5A mutants with 10-aa deletions in the region of aa 258 to 337, NS3 expression was detectable; thus, these NS5A mutants support viral genome replication. However, cells electroporated with CP7-388/NS5AΔ248-257 RNA showed an extremely low

FIG 3 Quantitation of RNA replication of bicistronic BVDV replicon NS5A derivatives. (A to C) MDBK cells were electroporated with bicistronic BVDV Bici-388 RLuc NS3-3′ RNAs and harvested into lysis buffer at 2, 24, and 30 h pe. Replication kinetics of the bicistronic RNAs were determined by *Renilla* luciferase activity in cell lysates at the time points indicated. Values for each time point, determined in triplicates, with corresponding standard deviations are shown in separate diagrams. Data are representative of two independent transcription/electroporation experiments. WT, BVDV Bici-388 RLuc NS3-3′ WT; GAA, BVDV Bici-388 RLuc NS3-3′ GAA; RLU, relative light units. The individual NS5A deletions in the BVDV Bici-388 RLuc NS3-3′ RNAs are specified by the *x* axis designations. Polymerase-defective RNA Bici-388 RLuc NS3-3′ GAA served as a negative control.

replication level indicated by very weak NS3 expression (Fig. 5A). In conclusion, the replication phenotypes of the individual CP7-388 NS5A mutants correlated well with replication capabilities of the NS5A mutants determined in the Bici-388 RLuc NS3-3′ system.

Cell culture supernatants of electroporated cells were harvested at 48 h pe and used to inoculate naive cells to determine the capability of the individual CP7-388 NS5A mutants to produce infectious virus particles. The production of infectious virus was determined via NS3-specific IF assay 72 h pi. Supernatants from cells electroporated with CP7-388 derivatives encoding NS5A mutants with deletions spanning aa 258 to 337 contained infectious BVDV particles, as indicated by the appearance of NS3-positive foci of infected cells. In contrast, no infectious virions could be detected in the supernatants of cells that had been electroporated with CP7-388/NS5AΔ248-257 RNA. To quantify the infectious particle formation capacity of these mutants, the supernatants of electroporated cells were titrated as described in Materials and Methods. Analysis of the amount of released infectious virus revealed a broad correlation with the observed replication phenotype (Fig. 5A and B): CP7-388 NS5A mutants 258-337 showed a drastic reduction in the production of infectious virus compared to CP7-388/WT (Fig. 5C). In conclusion, the obtained data show that CP7-388 derivatives encoding NS5A mutants with deletions spanning residues 258 to 337 are capable of producing infectious particles, but they do so at severely reduced titers. These observations support the conclusion that the decrease in produced virus titers for all tested viable NS5A mutations originates from inefficient viral RNA replication rather than from a specific disruption of virus assembly and/or virus release (Fig. 3B and C and 5C). This is best exemplified by the failure of CP7-388/NS5AΔ248-257 RNA to produce detectable amounts of virus particles. Along these lines, titer determination after an infection with a defined MOI of 0.05 further corroborated the observed reduction in the infectious particle production for all mutants tested. However, due to the very low titers obtained, titer determination was experimentally challenging (data not shown).

The fact that all viable NS5A deletion mutants (258-267 to 328-337) are somewhat impaired with respect to viral RNA replication (10- to 100-fold lower than the WT; Fig. 3B) makes it difficult to judge if the reduction in viral titers stemmed exclusively from the lower RNA replication efficiencies of the mutant viral replicase or whether RNA replication-independent effects on virion morphogenesis also contribute to the very low virus titers. To address this question, the quantification of viral RNA replication of full-length viral genomes would be necessary without the contributions of viral spread. Therefore, we introduced all viable NS5A deletions into a bicistronic BVDV RLuc-NS2-3′ RNA replicon. This NS2-3′ replicon RNA mimics the viral RNA replication phenotype of full-length viral genomes while avoiding viral spread due to the temporal regulation of the NS2-3 cleavage and the lack of the structural proteins. The NS2-3′ replicons harboring NS5A deletions 258-267 to 328-337 replicated 50- to 100-fold less efficiently than wild-type Bici-388 RLuc NS2-3′ at 24 h pe (Fig. 5D). After 48 h pe, the mutant replicon RNAs with NS5A deletions 258-267 to 328-337 showed a further increase in luciferase activity, while the RLuc activity in cells electroporated with the wild-type bicistronic replicon declined compared to the 24-h value, most likely due to the induced severe CPE. Therefore, comparison of the replication efficiencies of mutant replicon RNAs to that of the wild-type replicon RNA at the 48-h time point was compromised (Fig. 5D). The bicistronic NS2-3′ replicon with the 248-257 deletion did not replicate detectably at both time points, confirming the IF results after 48 h pe and very low titers detectable after 72 h pi (Fig. 5B, C, and D).

Overall, we observed a good correlation between replication efficiencies of these replicons and the obtained titers of the corresponding CP7 mutants, indicating that the low virus titers originate mainly from defects of the viral RNA replication process. However, we cannot rule out that certain deletions affect specific NS5A function(s) in the virus assembly process, thereby contributing to the low virus titers detected.

Furthermore, we tested whether the NS5A mutants that are severely impaired in RNA replication alter the secretion of viral RNA into supernatants of infected cells, e.g., whether these mutants release large quantities of noninfectious virus particles. To this end, we determined the amount of intracellular and extracellular viral RNA 30 and 48 h pe of the BVDV CP7 RNAs carrying NS5A deletion 258-267 or 298-307 and compared those values to the ones obtained with the CP7-388/WT RNA. We observed a strong correlation of intracellular and extracellular viral RNA levels with infectious titers, i.e., both mutants that showed reduced infectious titers by 2 logs or more compared to the WT also exhibit 1.5 to 2 logs or more decreased RNA quantities of intra- and extracellular viral RNA compared to the CP7-388/WT RNA (Fig. 6). Accordingly, none of the tested mutants showed a specific alteration in the relative amounts of secreted viral RNA. These results suggest that these NS5A mutations cause a defect upstream of the infectious virus particle release.

Establishment of a functional BVDV replicon expressing a fluorescent NS5A-mCherry protein. The results obtained demonstrated that monocistronic replicons with deletions in LCS I of NS5A still displayed rather robust RNA replication. Therefore, we inserted the gene coding for the mCherry fluorescent protein into the center of LCS I (Fig. 7A). In live cell microscopy, cells transfected with pT7-DI-388mCherry displayed NS5A-mCherry fluorescence (Fig. 7B). To check processing of the NS5A-mCherry fusion protein in the context of the polyprotein, vaccinia virus MVA-T7pol-based expression was performed in Huh7-T7 cells using plasmids pT7-DI-388/WT, pT7-DI-388/NS5AΔ288-297, and pT7-DI-388mCherry. In lysates of cells transfected with pT7-DI-388mCherry, Western blot analysis using a MAb directed against BVDV NS5A detected the NS5A-mCherry fusion protein at its expected molecular mass of approximately 80 kDa. The unmodified NS5A protein of approximately 55 kDa was detected only in pT7-DI-388/WT- and pT7-DI-388/NS5AΔ288-297-transfected cells (Fig. 7C). In addition, correctly processed NS3 and NS4A proteins were detected in cells transfected with all plasmids, including pT7-DI-388mCherry (Fig. 7C). According to this analysis, the insertion of mCherry into NS5A does not affect the processing of the viral polyprotein.

Based on this promising result, DI-388mCherry replicon RNA was *in vitro* transcribed and electroporated into MDBK cells, followed by immunofluorescence microscopy to monitor viral RNA replication and NS5A-mCherry expression. The detection of NS3-positive cells by indirect immunofluorescence microscopy using Alexa Fluor 488-labeled secondary antibodies at 48 h pe confirmed that the DI-388mCherry/WT RNA is capable of autonomous replication (Fig. 7D). Further analysis revealed that the NS3-positive cells were also positive for NS5A-mCherry expres-

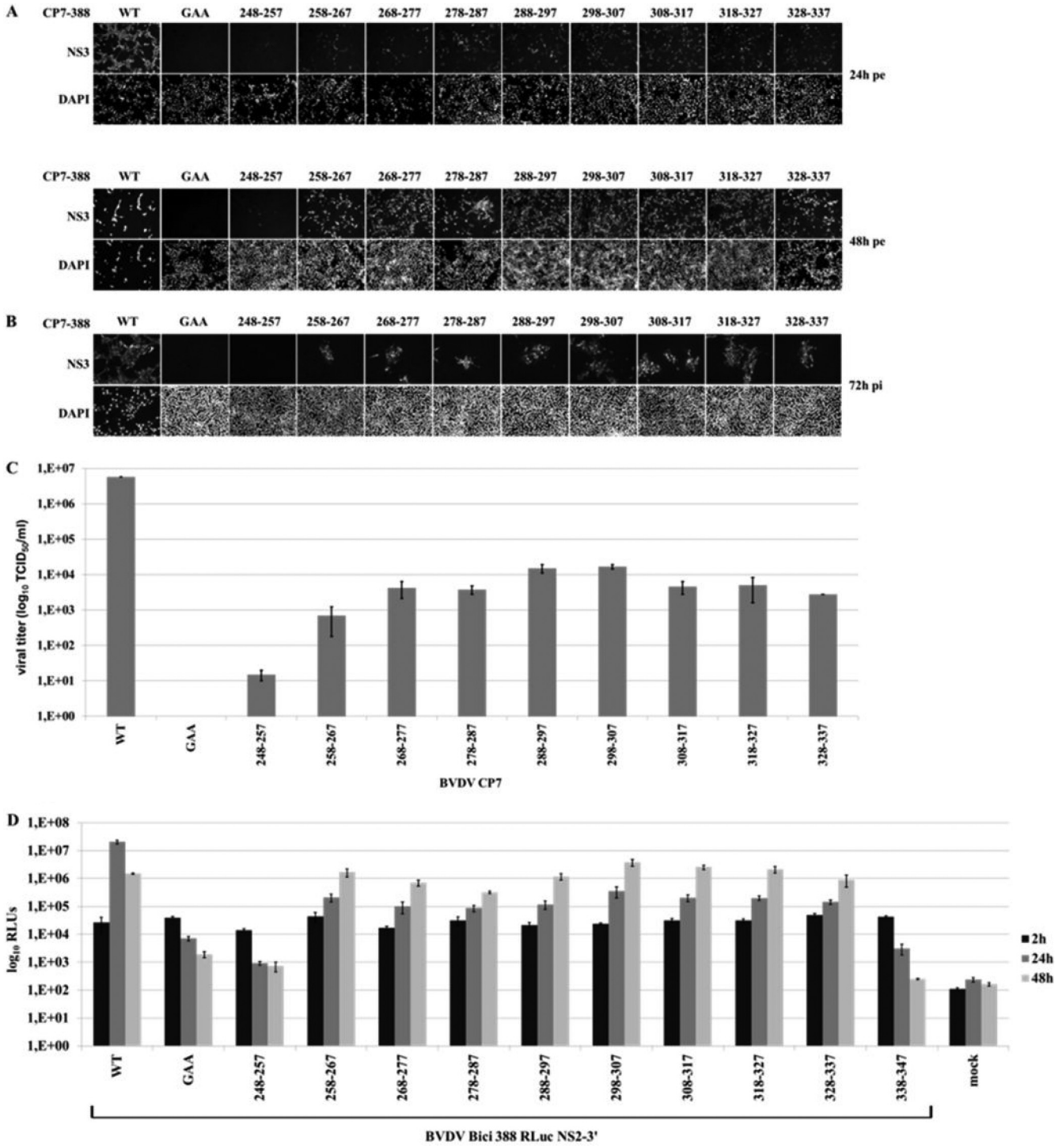

FIG 5 Impact of different NS5A mutations on BVDV production. (A) BVDV CP7-388 RNAs electroporated into MDBK cells are indicated above each IF image. Cells were fixed 24 and 48 h pe and analyzed for RNA replication by the NS3-specific IF assay (top rows, NS3). Nuclei were counterstained with DAPI (bottom rows, DAPI). (B) Supernatants from electroporated cells were harvested 48 h pe and used for inoculation of naive MDBK cells. The presence of infectious BVDV in the supernatant was determined at 72 h postinfection by NS3-specific immunofluorescence (top row, NS3). Nuclei of cells were stained with DAPI (bottom row, DAPI). (C) In parallel, infectivity of the supernatants of electroporated cells 48 h pe was determined as the 50% tissue culture infectious dose ($TCID_{50}$) at 72 h postinfection. Values of viral titers shown represent the means from two independent experiments, each measured in duplicate. (D) MDBK cells were electroporated with bicistronic BVDV Bici-388 RLuc NS2-3′ RNAs and harvested into lysis buffer at 2, 24, and 48 h pe. Replication kinetics of the bicistronic RNAs were determined by *Renilla* luciferase activity in cell lysates at the time points indicated. Values for each time point, determined in triplicates, with corresponding standard deviations are shown. Data are representative of two independent transcription/electroporation experiments. WT, BVDV Bici-388 RLuc NS3-3′ WT; GAA, BVDV Bici-388 RLuc NS3-3′ GAA; RLU, relative light units. The individual NS5A deletions in the BVDV Bici-388 RLuc NS2-3′ RNAs are specified by the *x* axis designations. Polymerase-defective RNA Bici-388 RLuc NS2-3′/GAA served as a negative control.

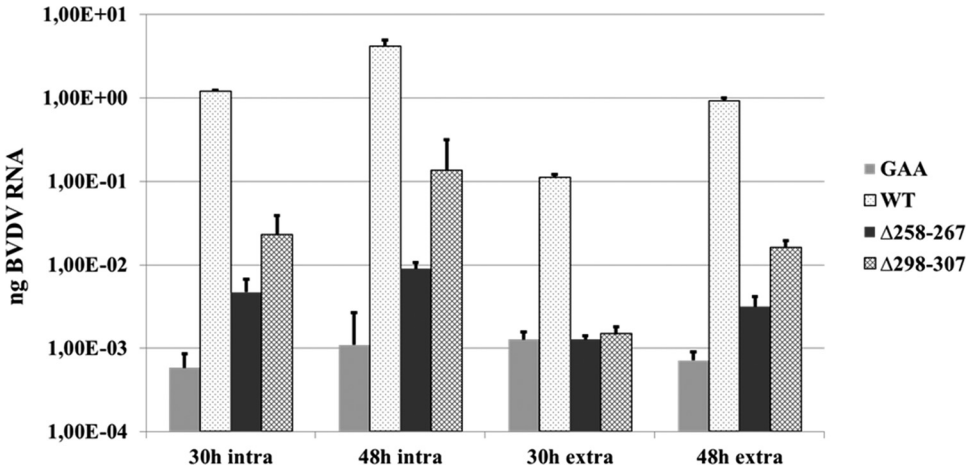

FIG 6 NS5A mutations do not alter the ratio of secreted viral RNA. MDBK cells were electroporated with wild-type or mutant CP7-388 RNAs, and intra- and extracellular viral RNA amounts were analyzed by quantitative real-time RT-PCR at the time points indicated. WT, wild type; GAA, replication-defective NS5B mutant; Δ258-267 and Δ298-307, CP7-388 NS5A deletion mutants. The experiment was performed in triplicates; results are depicted as mean values and standard deviations. The amount of the intracellular BVDV RNA is given in ng/10^6 cells, and the amount of extracellular viral RNA is given as ng/ml supernatant.

sion, as determined by fluorescence microscopy (Fig. 7D). Upon electroporation of the corresponding replication-deficient DI-388mCherry/GAA replicon RNA, no NS5A-mCherry fluorescence was detected (data not shown). This observation demonstrates that the NS5A-mCherry protein is functional in viral RNA replication; thus, it can be used to visualize BVDV RNA replication complexes by live cell imaging.

The insertion of other sequences into the center of LCS I yielded mixed results: while the insertion of a small sequence coding for the StrepII tag in the DI-388 replicon RNA allowed for viral RNA replication at rates similar to those of the wild type, the replacement of the mCherry coding sequence with that coding for the GFP in this replicon further decreased the replication efficiency compared to the DI-388mCherry replicon (data not shown). Further attempts to insert the mCherry coding sequence into the C-terminal region of domain III (e.g., replacing NS5A amino acids 479 to 488) failed to produce a viable replicon (data not shown).

BVDV NS5A localizes to lipid droplets. In cells electroporated with DI-388mCherry replicon RNA, we observed that a fraction of NS5A-mCherry formed ring-like structures that resembled nonadipocyte lipid droplets (LDs) based on their size of less than 1 μm in diameter (62). Previously, it has been shown that HCV NS5A gets recruited to LD structures (38). As Perilipin is a cellular protein residing at the surface of LDs (63), ectopic expression of eGFP-Perilipin was used to characterize the ring-like structures stained by NS5A-mCherry. To this end, MDBK cells were electroporated with DI-388mCherry replicon RNA and peGFP-N1-Perilipin. Live cell imaging analysis demonstrated a colocalization of eGFP-Perilipin with a fraction of NS5A-mCherry (Fig. 8A, top row). This finding could be corroborated by costaining MDBK cells replicating the DI-388mCherry RNA with the LD-specific dye Bodipy 493/503 (Fig. 8A, bottom row). Since NS5A is a known component of the viral replicase, we asked if other viral NS proteins were also localized to the surface of LD. To address this question, the DI-388mCherry replicating MDBK cells costained with Bodipy 493/503 were counterstained with an anti-NS3 antibody. This experiment revealed that (i) a larger proportion of NS5A-mCherry than NS3 is found at the surface of LDs (Fig. 8A, line plot, bottom row; compare the red and blue graphs near the LD indicated by the green graph) and (ii) a significant fraction of NS3 and NS5A-mCherry indeed colocalizes in cytoplasmic foci not stained positive for LDs (Fig. 8A, bottom row, see line plot), possibly representing viral replication complexes. However, further experiments are required to validate the latter assumption.

In a second approach, MDBK cells were first electroporated with DI-388mCherry replicon RNA and subsequently counterstained with the LD-specific dye Bodipy 493/503 prior to live cell microscopy 48 h pe. A fraction of BVDV NS5A-mCherry appeared to reside on the surface of the LD structures stained by Bodipy 493/503 (Fig. 8Bi). Moreover, NS5A-mCherry was also found at membrane structures in the periphery of the LDs (Fig. 8Bi).

In order to determine if expression of NS5A-mCherry alone leads to the observed LD association in the absence of other viral proteins, a pcDNA-NS5A-mCherry plasmid was electroporated into MDBK cells, and the cellular localization of NS5A-mCherry was monitored by live cell microscopy. The appearance of fluorescent ring-like structures upon NS5A-mCherry expression suggests that no additional viral proteins are required to target NS5A-mCherry to the LDs (Fig. 8Bii).

To verify that the LD localization observed with NS5A-mCherry was not artificially triggered by the mCherry insertion, the cellular localization of authentic NS5A was analyzed in cells that were either electroporated with DI-388 replicon RNA or infected with BVDV strain CP7. In these cells, NS5A was detected by a BVDV NS5A-specific IF assay, along with counterstaining of LDs by Bodipy 493/503. In accordance with the results obtained by live cell imaging of NS5A-mCherry, a fraction of authentic NS5A was found at the surface of LDs (Fig. 8B, compare i to ii and iii to iv).

DISCUSSION

NS5A is a phosphoprotein with a structural Zn-binding site in its N-terminal domain and serves essential, but not yet fully characterized, functions in RNA replication of BVDV (15–17). In this study, we carried out a systematic reverse genetic analysis of the

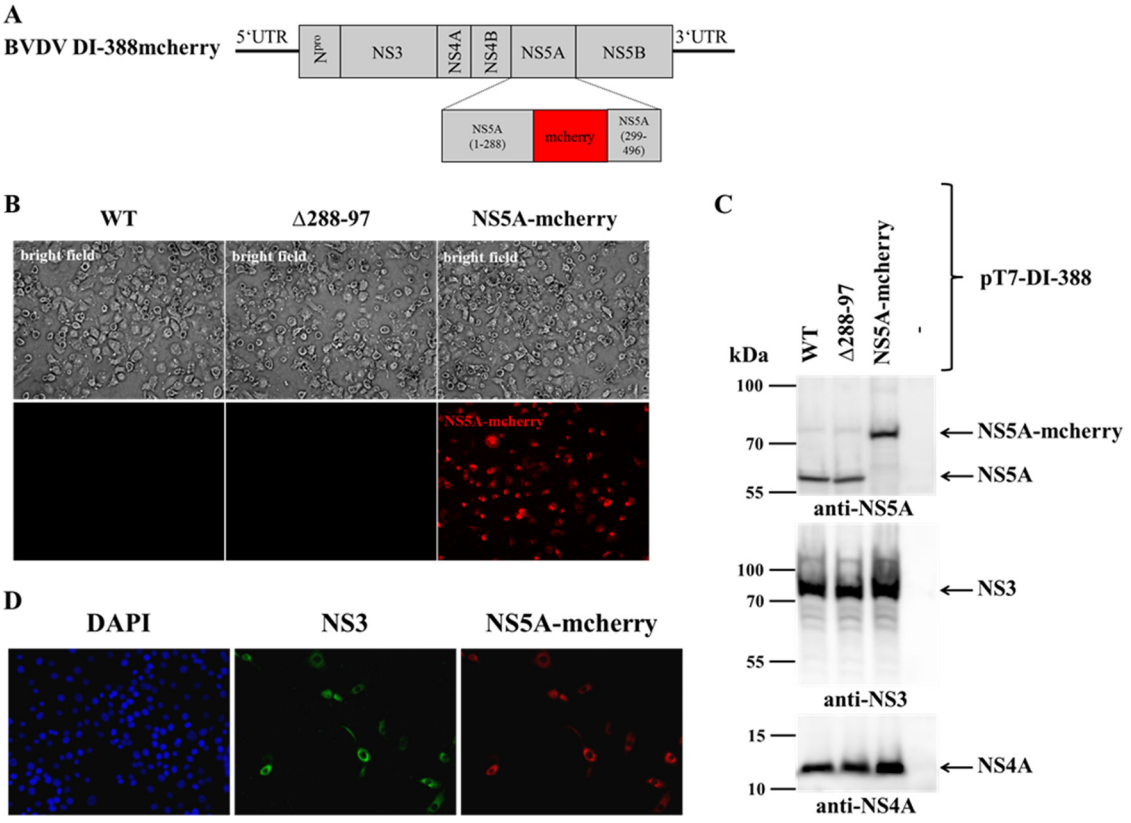

FIG 7 Establishment of a BVDV DI-388mCherry replicon. (A) Schematic representation of the BVDV DI-388mCherry replicon. The mCherry coding sequence was introduced after amino acid 288 of NS5A (numbering refers to BVDV CP7 NS5A). The resulting organization of NS5A-mCherry is shown below. (B) Visualization of fluorescent NS5A-mCherry. Huh7-T7 cells were infected with vaccinia virus MVA-T7pol and transfected with pT7-DI-388, pT7-DI-388Δ288-297, or pT7-DI-388mCherry. Live cell images were acquired 24 h posttransfection. (C) NS5A-mCherry does not affect polyprotein processing. Transfected cells used for live cell imaging were harvested 24 h posttransfection and analyzed for NS3, NS4A, and NS5A/NS5A-mCherry expression by Western blotting. (D) The BVDV DI-388mCherry RNA is replication competent. MDBK cells electroporated with BVDV DI-388mCherry replicon RNA were fixed at 48 h pe. Cells were stained with NS3-specific antibody and a secondary Alexa Fluor 488-labeled antibody (center). NS5A-mCherry was directly visualized by fluorescence microscopy (right). Nuclei were counterstained with DAPI (left).

C-terminal half of the NS5A protein to determine its functional importance in the pestiviral life cycle. The minimal set of viral proteins required for RNA replication of pestiviruses is the NS3 to NS5B region of the polyprotein. It is also known that uncleaved NS2-3 cannot substitute for NS3 in this process, and that generation of the authentic N terminus of NS3 is essential for RNA amplification. In the context of the viral full-length polyprotein, the NS2 autoprotease, in conjunction with a cellular chaperone as its cofactor, regulates the amount of free NS3 and thereby viral RNA replication efficiency (54, 64, 65). Due to this mechanism and the differences in genome size, full-length BVDV genomes replicate with a significantly lower efficiency than DI-388 replicon RNA. This difference is best exemplified by the observed onset of a CPE in MDBK cells; while the full-length genome of the cytopathogenic BVDV strain CP7 causes a severe CPE around 48 h pe, cells replicating the DI-388 replicon RNA start to develop a CPE as early as 16 h pe. The bicistronic Bici-388 RLuc NS3-3′ replicon RNA replicates at an intermediate level in MDBK cells with CPE detectable around 24 h pe (Fig. 3, compare the decrease in RLuc activity for Bici-388 RLuc NS3-3′ WT at the 24- and 30-h time points). These differences in RNA replication efficiency are also reflected in the results obtained in the NS5A deletion mutagenesis study. While the deletions introduced in the NS5A region encompassing aa 438 to 488 allowed for low-level RNA replication in the context of the most efficient replicon, DI-388 (Fig. 2), no viral RNA replication was detectable when the same set of deletions was tested in the context of the Bici-388 RLuc NS3-3′ replicon or the full-length CP7-388 viral genome (Fig. 3 and data not shown). In contrast, the deletions spanning the NS5A region of aa 258 to 337 were tolerated in the context of all three applied viral RNA species and gave rise to intermediate levels of viral RNA replication and a small but detectable amount of virion production (Fig. 2, 3, and 5). Deletion of NS5A amino acids 248 to 257 produced only a very low level of RNA replication upon electroporation of the corresponding RNAs (Fig. 2, 3, and 5, compare 248-257 to 258-267), suggesting that this region is in close proximity to the essential domain I. In summary, the data presented provide a comprehensive functional map of the C-terminal half of BVDV NS5A with respect to viral RNA replication and virion production. The results suggest that most of the putative LCS I, as well as the N-terminal part of the domain II between NS5A aa 258 and 337, is essential for neither RNA replication nor virion morphogenesis. However, we should stress that the ability of all of these deletion mutants to replicate or to produce infectious virus is strongly reduced compared to the respective wild-type situations (Fig. 2, 3, and 5). A specific block of viral RNA secretion into the superna-

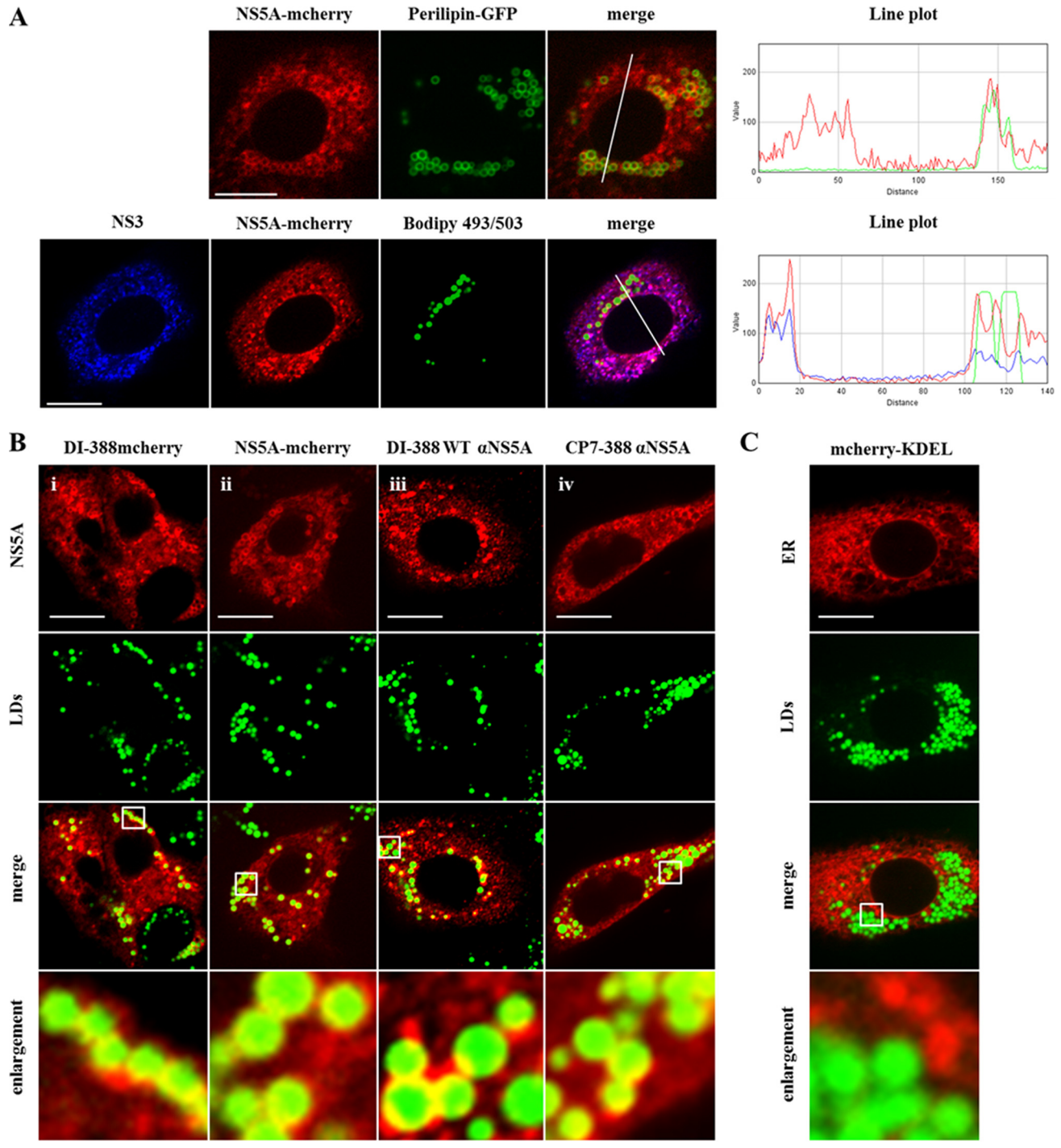

FIG 8 A fraction of NS5A localizes to the surface of lipid droplets. (A) In the top row, NS5A-mCherry colocalizes with Perilipin-GFP at lipid droplets. MDBK cells were coelectroporated with BVDV DI-388mCherry RNA and peGFP-N1-Perilipin. Fluorescent proteins were visualized 48 h pe by confocal live cell imaging as indicated (scale bar, 10 μm). LD localization was visualized with the recognized LD marker eGFP-Perilipin (green). The line plot (right) shows intensity values for both NS5A-mCherry (red graph) and eGFP-Perilipin (green graph) along the line drawn across the merged image. In the bottom row are confocal images of MDBK cells electroporated with BVDV DI-388mCherry replicon RNA 48 h pe. NS5A-mCherry was directly visualized by fluorescence microscopy (red). LD localization is indicated by Bodipy 493/503 (green). NS3 was visualized using an NS3-specific antibody and a secondary Alexa Fluor 647-labeled antibody (blue). The line plot (right) shows intensity values for NS5A-mCherry (red graph), LDs (green graph), and NS3 (blue graph) along the line drawn across the merged image. (B) Confocal microscopy-aided detection of NS5A-mCherry and NS5A at LDs within MDBK cells. NS5A was visualized with NS5A-mCherry fluorescence via live cell imaging (i and ii) or by indirect immunofluorescence with an NS5A-specific monoclonal antibody and a Cy3-labeled secondary antibody (iii and iv). LDs were stained with Bodipy 493/503 (green). The white box in each merged image indicates the enlarged section shown below. (i and ii) Live cell images of cells electroporated with the replicon DI-388mCherry 48 h pe and of cells expressing NS5A-mCherry 24 h pe. (iii and iv) Immunofluorescence images of cells containing DI-388, cells fixed 18 h pe, or CP7-388, cells fixed 48 h pi. (C) Confocal microscopy live cell image of MDBK cells, endoplasmic reticulum visualized with mCherry-KDEL (red), and lipid droplets stained with Bodipy 493/503 (green) served as controls, i.e., for noncolocalization to LDs. Scale bars, 10 μm.

tant could not be observed for any of the tested NS5A mutants (Fig. 6). This indicates that the deletions affect a step in viral replication upstream of virion release. For a better understanding it will be interesting to identify possible second-site mutations that rescue RNA replication and/or virion morphogenesis.

The remainder of the putative domain II of NS5A plays a pivotal role in RNA replication, since this region was essential in all of our test systems. Analysis of domain III mutants revealed that this region is not absolutely mandatory, since deletions are tolerated in the context of the DI-388 replicon, but this domain was essential in the CP7-388 context. Taking these findings together, domain III may contribute to the establishment of an efficient RNA replicase rather than serving essential functions of NS5A. As with all RNA viruses, the possible contribution of conserved secondary RNA structures to RNA replication has to be considered. Thus, we cannot exclude that the effect of individual deleterious mutations is based on alteration of critical RNA structures.

When comparing the contribution of domains II and III of HCV NS5A to viral RNA replication and virion morphogenesis, our findings reveal interesting parallels but also notable differences between the NS5A proteins of both viruses. First, the putative LCS I region and the N-terminal part of domain II of both NS5A proteins tolerate small deletions in RNA replication (37, 66). Second, different portions of the C-terminal part of domain II are critical for RNA replication in both virus systems: a region of 90 aa is essential for BVDV RNA replication (Fig. 2), while HCV RNA replication requires either the C-terminal 35 aa (HCV genotype 2a) or 56 aa (HCV genotype 1b) (37, 66, 67). Third, while large parts of HCV NS5A domain III can be deleted without affecting RNA replication, the putative domain III of BVDV NS5A is critical for pestiviral genome replication (Fig. 3 and data not shown) (33, 35–37, 66). Our reverse genetic analysis revealed a broad correlation between genome replication and virion morphogenesis for all tested deletion mutants (Fig. 5 and data not shown). Therefore, we cannot address the question of whether BVDV NS5A regions exist which specifically contribute to virus production. Such a pivotal role in virion morphogenesis has recently been demonstrated for HCV NS5A domain III (36, 66, 68, 69).

The observation that none of the tested NS5A deletion mutants caused any obvious disruptions of polyprotein translation and/or processing suggests that the inhibitory NS5A mutations interfere with specific functions of NS5A within the viral RNA replicase (Fig. 4). However, with the data available we cannot rule out that more subtle changes in processing kinetics, which are not detectable in our translation/processing system, inhibit viral RNA replication. In our analysis the NS5A-specific antibody recognized full-length NS5A with an apparent molecular mass of 55 kDa and also a less prominent additional protein of about 40 kDa. This protein was not detected upon expression of mutant polyproteins with deletions of NS5A aa 288 to 307 in the center of LCS I. One possible explanation for this observation is that the deletion of the central part of LCS I renders NS5A less accessible for cellular proteases or causes a reduced accessibility for an additional specific processing event by the NS3-4A protease. In any case, the fact that full-length genomes with deletions of NS5A aa 288 to 307 were still capable of RNA replication and virion morphogenesis suggests that generation of the 40-kDa fragment is not essential for these processes.

Recently, CSFV NS5A has been shown to regulate viral RNA replication by either binding to the 3′ UTR or interacting with NS5B (19). In their study, Chen and coworkers identified three regions (amino acids 137 to 172, 224 to 268, and 390 to 414) within NS5A that are required for NS5B binding. While the first two regions were also important for regulation of viral RNA synthesis, the region of aa 390 to 414 was nonessential for this regulation (19). Within these NS5A regions the authors identified 5 individual amino acids (W143, V145, P227, T246, and P257) that were critical for RNA replication in cell culture and 4 amino acids (K399, T401, E406, and L413) that were important for IRES-mediated translation and NS5B binding (19). Interestingly, these amino acids were found to be conserved between pestiviral and HCV NS5A. According to our present study, two of the identified CSFV NS5A regions (aa 137 to 172 and 224 to 268) would reside in domain I (aa 1 to 248) or overlap the putative LCS I (aa 249 to 282). Although we have not introduced deletions into domain I, the identification of CSFV NS5A P257 as being important for the NS5A-NS5B interaction as well as for viral replication by Chen et al. is corroborated by our observation that deleting aa 248 to 257 of BVDV NS5A strongly compromises NS5A function (Fig. 2, 3, and 5) (19). In contrast to the finding of Chen and coworkers that the third NS5B interaction region of NS5A (aa 390 to 414) is not essential for viral RdRp regulation *in vitro*, we observed that individual deletions of BVDV NS5A aa 338 to 437 strongly interfere with viral RNA replication in all of our test systems (Fig. 2 and 3 and data not shown). Furthermore, the authors could show that all nine amino acid residues are critical for viral RNA replication when mutated individually to alanine in the CSFV viral genome (19). This observation is in good agreement with the essential function of domain I and our finding that the C-terminal part of domain II and the entire domain III are critical for pestiviral RNA replication.

Previously, a negative regulatory effect of NS5A on CSFV IRES-mediated translation of a reporter mRNA was reported (20). This effect also depended on residues in the CSFV NS5A region of aa 390 to 414. However, we could not observe a similar regulatory effect of deletions in the corresponding region of BVDV NS5A on the IRES-mediated translation efficiencies of our different replicon RNAs (Fig. 3). The differences in the observations are likely due to the individual test systems used in the two studies.

The identification of the nonessential nature of the LCS I region enabled us to develop an RNA replicon expressing fluorescent NS5A-mCherry in the context of a functional pestiviral replicase. The fact that NS5A-mCherry could be detected no earlier than 48 h pe indicates that replication of this insertion mutant is rather inefficient. In fact, when the mCherry coding sequence was introduced into the bicistronic Bici-388 RLuc NS3-3′ replicon/Δ288-298 RNA, replication efficiency was further decreased 10-fold at 48 h pe compared to the parental Bici-388 RLuc NS3-3′ Δ288-298 replicon (data not shown). Using this novel tool, the cellular localization of NS5A-mCherry could be determined by live cell imaging. Interestingly, a fraction of NS5A-mCherry was localized at ring-like membranous structures identified as LDs by eGFP-Perilipin colocalization and Bodipy 493/503 staining (Fig. 8). The ability to visualize NS5A in living cells is especially helpful, since membrane structures are difficult to preserve when common antibody staining protocols are applied. In the HCV system, it was described that the viral core protein is targeted to LDs (39, 70). Moreover, NS5A, together with NS3, NS5B, and TIP47, is also targeted to the surface of LDs, and an NS5A-core protein interac-

tion at the LD surface is assumed to trigger an early step in the HCV virion assembly process (38, 66, 71, 72). *In vitro* analysis demonstrated that an N-terminal amphipathic helix of HCV NS5A serves as a membrane anchor and that an analogous helix present at the N terminus of BVDV NS5A can functionally replace that of HCV (21). In the present study, it was observed that a fraction of BVDV NS5A-mCherry resides at the surface of LDs when expressed either in the context of DI-388/NS5A-mCherry or from plasmid DNA; i.e, in the absence of the other viral proteins (Fig. 8). This localization mirrors the authentic cellular distribution of NS5A as confirmed by NS5A-specific antibody staining in cells either electroporated with replicon DI-388 or infected with BVDV CP7. However, without quantitative data, we cannot exclude that the presence of other pestiviral proteins causes an even more efficient targeting of NS5A to LDs. While colocalization of NS5A with NS3 was observed in cytoplasmic foci, NS5A but not NS3 appears to be enriched at the LD surface (Fig. 8A). This indicates that different NS5A protein complexes exist in infected cells, serving distinct function(s) throughout the viral life cycle.

Recently, it was observed that a CSFV mutant with a rescue mutation in the C-terminal part of NS3 can generate infectious progeny despite an almost complete deletion of the viral core protein (73, 74). This result implies that the core protein plays a minor role in the recruitment of the viral components which are involved in virion morphogenesis in the pestivirus system. Therefore, the results presented here raise the question of whether other pestiviral proteins localize at LDs.

The data obtained in this study highlight the importance of the NS5A protein in the pestiviral life cycle. Furthermore, this and other studies in the CSFV system (19) contribute to a better understanding of remarkable common features of the NS5A proteins of pestiviruses and HCV, such as their localization to the surface of LDs, their importance for viral RNA replication, and their role in modulating the viral replicase complex.

ACKNOWLEDGMENTS

We especially thank B. Bruhn, S. Schwindt, and M. Alexander for excellent technical assistance. We also thank Lars Krüger for contributions in the initial phase of this project. We are grateful to E. J. Dubovi (Cornell University, Ithaca, NY) for antibody 8.12.7, directed against BVDV NS3, S. Lemon (UNC, Chapel Hill, NC) for providing us with the Huh7-T7 cell line, and G. Sutter (LMU, Munich, Germany) for the MVA-T7 vaccinia virus stock. We thank A. Palmenberg (University of Wisconsin, Madison, WI) for the pF/R-wt plasmid, G. Voeltz (University of Colorado, CO) for the pmCherry-KDEL plasmid, and H. Heid (German Cancer Center, Heidelberg, Germany) for the peGFP-N1 Perilipin plasmid. We also thank B. Wölk (Hannover Medical School, Hannover, Germany) for advice and members of the Tautz group for helpful discussion.

This work was supported by intramural funding from the University of Lübeck (N.T.) and a grant from the DFG Excellence Cluster "Inflammation at Interfaces" (R.D.).

REFERENCES

1. **Stapleton JT, Foung S, Muerhoff AS, Bukh J, Simmonds P.** 2011. The GB viruses: a review and proposed classification of GBV-A, GBV-C (HGV), and GBV-D in genus Pegivirus within the family Flaviviridae. J. Gen. Virol. **92:**233–246. http://dx.doi.org/10.1099/vir.0.027490-0.
2. **Lindenbach BD, Thiel H-J, Rice CM.** 2007. Flaviviridae: the viruses and their replication, p 1101–1152. *In* Knipe DM, Howley PM (ed), Fields virology, 5th ed, vol 1. Lippincott Williams & Wilkins, Philadelphia, PA.
3. **Chon SK, Perez DR, Donis RO.** 1998. Genetic analysis of the internal ribosome entry segment of bovine viral diarrhea virus. Virology **251:**370–382. http://dx.doi.org/10.1006/viro.1998.9425.
4. **Murray CL, Jones CT, Rice CM.** 2008. Architects of assembly: roles of Flaviviridae non-structural proteins in virion morphogenesis. Nat. Rev. Microbiol. **6:**699–708. http://dx.doi.org/10.1038/nrmicro1928.
5. **Behrens S-E, Grassmann CW, Thiel H-J, Meyers G, Tautz N.** 1998. Characterization of an autonomous subgenomic pestivirus RNA replicon. J. Virol. **72:**2364–2372.
6. **Myers TM, Kolupaeva VG, Mendez E, Baginski SG, Frolov I, Hellen CU, Rice CM.** 2001. Efficient translation initiation is required for replication of bovine viral diarrhea virus subgenomic replicons. J. Virol. **75:**4226–4238. http://dx.doi.org/10.1128/JVI.75.9.4226-4238.2001.
7. **Tautz N, Harada T, Kaiser A, Rinck G, Behrens SE, Thiel H-J.** 1999. Establishment and characterization of cytopathogenic and noncytopathogenic pestivirus replicons. J. Virol. **73:**9422–9432.
8. **Tautz N, Thiel H-J.** 2003. Cytopathogenicity of pestiviruses: cleavage of bovine viral diarrhea virus NS2-3 has to occur at a defined position to allow viral replication. Arch. Virol. **148:**1405–1412.
9. **Tautz N, Thiel HJ, Dubovi EJ, Meyers G.** 1994. Pathogenesis of mucosal disease: a cytopathogenic pestivirus generated by an internal deletion. J. Virol. **68:**3289–3297.
10. **Xu J, Mendez E, Caron PR, Lin C, Murcko MA, Collett MS, Rice CM.** 1997. Bovine viral diarrhea virus NS3 serine proteinase: polyprotein cleavage sites, cofactor requirements, and molecular model of an enzyme essential for pestivirus replication. J. Virol. **71:**5312–5322.
11. **Grassmann CW, Isken O, Behrens SE.** 1999. Assignment of the multifunctional NS3 protein of bovine viral diarrhea virus during RNA replication: an in vivo and in vitro study. J. Virol. **73:**9196–9205.
12. **Kao CC, Del Vecchio AM, Zhong W.** 1999. De novo initiation of RNA synthesis by a recombinant flaviviridae RNA-dependent RNA polymerase. Virology **253:**1–7. http://dx.doi.org/10.1006/viro.1998.9517.
13. **Steffens S, Thiel H-J, Behrens S-E.** 1999. The RNA-dependent RNA polymerases of different members of the family Flaviviridae exhibit similar properties in vitro. J. Gen. Virol. **80:**2583–2590.
14. **Hanoulle X, Badillo A, Verdegem D, Penin F, Lippens G.** 2010. The domain 2 of the HCV NS5A protein is intrinsically unstructured. Protein Pept. Lett. **17:**1012–1018. http://dx.doi.org/10.2174/092986610791498920.
15. **Reed KE, Gorbalenya AE, Rice CM.** 1998. The NS5A/NS5 proteins of viruses from three genera of the family flaviviridae are phosphorylated by associated serine/threonine kinases. J. Virol. **72:**6199–6206.
16. **Tellinghuisen TL, Paulson MS, Rice CM.** 2006. The NS5A protein of bovine viral diarrhea virus contains an essential zinc-binding site similar to that of the hepatitis C virus NS5A protein. J. Virol. **80:**7450–7458. http://dx.doi.org/10.1128/JVI.00358-06.
17. **Grassmann CW, Isken O, Tautz N, Behrens SE.** 2001. Genetic analysis of the pestivirus nonstructural coding region: defects in the NS5A unit can be complemented in trans. J. Virol. **75:**7791–7802. http://dx.doi.org/10.1128/JVI.75.17.7791-7802.2001.
18. **Sapay N, Montserret R, Chipot C, Brass V, Moradpour D, Deleage G, Penin F.** 2006. NMR structure and molecular dynamics of the in-plane membrane anchor of nonstructural protein 5A from bovine viral diarrhea virus. Biochemistry **45:**2221–2233. http://dx.doi.org/10.1021/bi0517685.
19. **Chen Y, Xiao J, Sheng C, Wang J, Jia L, Zhi Y, Li G, Chen J, Xiao M.** 2012. Classical swine fever virus NS5A regulates viral RNA replication through binding to NS5B and 3′UTR. Virology **432:**376–388. http://dx.doi.org/10.1016/j.virol.2012.04.014.
20. **Xiao M, Wang Y, Zhu Z, Yu J, Wan L, Chen J.** 2009. Influence of NS5A protein of classical swine fever virus (CSFV) on CSFV internal ribosome entry site-dependent translation. J. Gen. Virol. **90:**2923–2928. http://dx.doi.org/10.1099/vir.0.014472-0.
21. **Brass V, Pal Z, Sapay N, Deleage G, Blum HE, Penin F, Moradpour D.** 2007. Conserved determinants for membrane association of nonstructural protein 5A from hepatitis C virus and related viruses. J. Virol. **81:**2745–2757. http://dx.doi.org/10.1128/JVI.01279-06.
22. **Gosert R, Jendrsczok W, Berke JM, Brass V, Blum HE, Moradpour D.** 2005. Characterization of nonstructural protein membrane anchor deletion mutants expressed in the context of the hepatitis C virus polyprotein. J. Virol. **79:**7911–7917. http://dx.doi.org/10.1128/JVI.79.12.7911-7917.2005.
23. **Tellinghuisen TL, Marcotrigiano J, Gorbalenya AE, Rice CM.** 2004. The NS5A protein of hepatitis C virus is a zinc metalloprotein. J. Biol. Chem. **279:**48576–48587. http://dx.doi.org/10.1074/jbc.M407787200.
24. **Tellinghuisen TL, Marcotrigiano J, Rice CM.** 2005. Structure of the zinc-binding domain of an essential component of the hepatitis C virus replicase. Nature **435:**374–379. http://dx.doi.org/10.1038/nature03580.

25. **Foster TL, Belyaeva T, Stonehouse NJ, Pearson AR, Harris M.** 2010. All three domains of the hepatitis C virus nonstructural NS5A protein contribute to RNA binding. J. Virol. **84:**9267–9277. http://dx.doi.org/10.1128/JVI.00616-10.
26. **Huang L, Hwang J, Sharma SD, Hargittai MR, Chen Y, Arnold JJ, Raney KD, Cameron CE.** 2005. Hepatitis C virus nonstructural protein 5A (NS5A) is an RNA-binding protein. J. Biol. Chem. **280:**36417–36428. http://dx.doi.org/10.1074/jbc.M508175200.
27. **Chatterji U, Bobardt M, Selvarajah S, Yang F, Tang H, Sakamoto N, Vuagniaux G, Parkinson T, Gallay P.** 2009. The isomerase active site of cyclophilin A is critical for hepatitis C virus replication. J. Biol. Chem. **284:**16998–17005. http://dx.doi.org/10.1074/jbc.M109.007625.
28. **Kaul A, Stauffer S, Berger C, Pertel T, Schmitt J, Kallis S, Zayas M, Lohmann V, Luban J, Bartenschlager R.** 2009. Essential role of cyclophilin A for hepatitis C virus replication and virus production and possible link to polyprotein cleavage kinetics. PLoS Pathog. **5:**e1000546. http://dx.doi.org/10.1371/journal.ppat.1000546.
29. **Liu Z, Yang F, Robotham JM, Tang H.** 2009. Critical role of cyclophilin A and its prolyl-peptidyl isomerase activity in the structure and function of the hepatitis C virus replication complex. J. Virol. **83:**6554–6565. http://dx.doi.org/10.1128/JVI.02550-08.
30. **Verdegem D, Badillo A, Wieruszeski JM, Landrieu I, Leroy A, Bartenschlager R, Penin F, Lippens G, Hanoulle X.** 2011. Domain 3 of NS5A protein from the hepatitis C virus has intrinsic alpha-helical propensity and is a substrate of cyclophilin A. J. Biol. Chem. **286:**20441–20454. http://dx.doi.org/10.1074/jbc.M110.182436.
31. **Watashi K, Ishii N, Hijikata M, Inoue D, Murata T, Miyanari Y, Shimotohno K.** 2005. Cyclophilin B is a functional regulator of hepatitis C virus RNA polymerase. Mol. Cell **19:**111–122. http://dx.doi.org/10.1016/j.molcel.2005.05.014.
32. **Yang F, Robotham JM, Grise H, Frausto S, Madan V, Zayas M, Bartenschlager R, Robinson M, Greenstein AE, Nag A, Logan TM, Bienkiewicz E, Tang H.** 2010. A major determinant of cyclophilin dependence and cyclosporine susceptibility of hepatitis C virus identified by a genetic approach. PLoS Pathog. **6:**e1001118. http://dx.doi.org/10.1371/journal.ppat.1001118.
33. **Appel N, Pietschmann T, Bartenschlager R.** 2005. Mutational analysis of hepatitis C virus nonstructural protein 5A: potential role of differential phosphorylation in RNA replication and identification of a genetically flexible domain. J. Virol. **79:**3187–3194. http://dx.doi.org/10.1128/JVI.79.5.3187-3194.2005.
34. **Moradpour D, Evans MJ, Gosert R, Yuan Z, Blum HE, Goff SP, Lindenbach BD, Rice CM.** 2004. Insertion of green fluorescent protein into nonstructural protein 5A allows direct visualization of functional hepatitis C virus replication complexes. J. Virol. **78:**7400–7409. http://dx.doi.org/10.1128/JVI.78.14.7400-7409.2004.
35. **Liu S, Ansari IH, Das SC, Pattnaik AK.** 2006. Insertion and deletion analyses identify regions of non-structural protein 5A of hepatitis C virus that are dispensable for viral genome replication. J. Gen. Virol. **87:**323–327. http://dx.doi.org/10.1099/vir.0.81407-0.
36. **Tellinghuisen TL, Foss KL, Treadaway J.** 2008. Regulation of hepatitis C virion production via phosphorylation of the NS5A protein. PLoS Pathog. **4:**e1000032. http://dx.doi.org/10.1371/journal.ppat.1000032.
37. **Tellinghuisen TL, Foss KL, Treadaway JC, Rice CM.** 2008. Identification of residues required for RNA replication in domains II and III of the hepatitis C virus NS5A protein. J. Virol. **82:**1073–1083. http://dx.doi.org/10.1128/JVI.00328-07.
38. **Miyanari Y, Atsuzawa K, Usuda N, Watashi K, Hishiki T, Zayas M, Bartenschlager R, Wakita T, Hijikata M, Shimotohno K.** 2007. The lipid droplet is an important organelle for hepatitis C virus production. Nat. Cell Biol. **9:**1089–1097. http://dx.doi.org/10.1038/ncb1631.
39. **Moradpour D, Englert C, Wakita T, Wands JR.** 1996. Characterization of cell lines allowing tightly regulated expression of hepatitis C virus core protein. Virology **222:**51–63. http://dx.doi.org/10.1006/viro.1996.0397.
40. **Shi ST, Polyak SJ, Tu H, Taylor DR, Gretch DR, Lai MM.** 2002. Hepatitis C virus NS5A colocalizes with the core protein on lipid droplets and interacts with apolipoproteins. Virology **292:**198–210. http://dx.doi.org/10.1006/viro.2001.1225.
41. **Barba G, Harper F, Harada T, Kohara M, Goulinet S, Matsuura Y, Eder G, Schaff Z, Chapman MJ, Miyamura T, Brechot C.** 1997. Hepatitis C virus core protein shows a cytoplasmic localization and associates to cellular lipid storage droplets. Proc. Natl. Acad. Sci. U. S. A. **94:**1200–1205. http://dx.doi.org/10.1073/pnas.94.4.1200.
42. **Masaki T, Suzuki R, Murakami K, Aizaki H, Ishii K, Murayama A, Date T, Matsuura Y, Miyamura T, Wakita T, Suzuki T.** 2008. Interaction of hepatitis C virus nonstructural protein 5A with core protein is critical for the production of infectious virus particles. J. Virol. **82:**7964–7976. http://dx.doi.org/10.1128/JVI.00826-08.
43. **Kim CS, Jung JH, Wakita T, Yoon SK, Jang SK.** 2007. Monitoring the antiviral effect of alpha interferon on individual cells. J. Virol. **81:**8814–8820. http://dx.doi.org/10.1128/JVI.02824-06.
44. **Schaller T, Appel N, Koutsoudakis G, Kallis S, Lohmann V, Pietschmann T, Bartenschlager R.** 2007. Analysis of hepatitis C virus superinfection exclusion by using novel fluorochrome gene-tagged viral genomes. J. Virol. **81:**4591–4603. http://dx.doi.org/10.1128/JVI.02144-06.
45. **Wölk B, Buchele B, Moradpour D, Rice CM.** 2008. A dynamic view of hepatitis C virus replication complexes. J. Virol. **82:**10519–10531. http://dx.doi.org/10.1128/JVI.00640-08.
46. **Wölk B, Sansonno D, Krausslich HG, Dammacco F, Rice CM, Blum HE, Moradpour D.** 2000. Subcellular localization, stability, and trans-cleavage competence of the hepatitis C virus NS3-NS4A complex expressed in tetracycline-regulated cell lines. J. Virol. **74:**2293–2304. http://dx.doi.org/10.1128/JVI.74.5.2293-2304.2000.
47. **Schultz DE, Honda M, Whetter LE, McKnight KL, Lemon SM.** 1996. Mutations within the 5′ nontranslated RNA of cell culture-adapted hepatitis A virus which enhance cap-independent translation in cultured African green monkey kidney cells. J. Virol. **70:**1041–1049.
48. **Sutter G, Ohlmann M, Erfle V.** 1995. Non-replicating vaccinia vector efficiently expresses bacteriophage T7 RNA polymerase. FEBS Lett. **371:**9–12. http://dx.doi.org/10.1016/0014-5793(95)00843-X.
49. **Pankraz A, Thiel HJ, Becher P.** 2005. Essential and nonessential elements in the 3′ nontranslated region of Bovine viral diarrhea virus. J. Virol. **79:**9119–9127. http://dx.doi.org/10.1128/JVI.79.14.9119-9127.2005.
50. **Corapi WV, Donis RO, Dubovi EJ.** 1990. Characterization of a panel of monoclonal antibodies and their use in the study of the antigenic diversity of bovine viral diarrhea virus. Am. J. Vet. Res. **51:**1388–1394.
51. **Lamp B, Riedel C, Roman-Sosa G, Heimann M, Jacobi S, Becher P, Thiel H-J, Rümenapf T.** 2011. Biosynthesis of classical swine fever virus nonstructural proteins. J. Virol. **85:**3607–3620. http://dx.doi.org/10.1128/JVI.02206-10.
52. **Meyers G, Tautz N, Becher P, Thiel H-J, Kümmerer B.** 1996. Recovery of cytopathogenic and noncytopathogenic bovine viral diarrhea viruses from cDNA constructs. J. Virol. **70:**8606–8613.
53. **Bochkov YA, Palmenberg AC.** 2006. Translational efficiency of EMCV IRES in bicistronic vectors is dependent upon IRES sequence and gene location. Biotechniques **41:**283–288. http://dx.doi.org/10.2144/000112243.
54. **Lackner T, Müller A, König M, Thiel H-J, Tautz N.** 2005. Persistence of bovine viral diarrhea virus is determined by a cellular cofactor of a viral autoprotease. J. Virol. **79:**9746–9755. http://dx.doi.org/10.1128/JVI.79.15.9746-9755.2005.
55. **Schägger H, von Jagow G.** 1987. Tricine-sodium dodecyl sulfate-polyacrylamide gel electrophoresis for the separation of proteins in the range from 1 to 100 kDa. Anal. Biochem. **166:**368–379. http://dx.doi.org/10.1016/0003-2697(87)90587-2.
56. **Lattwein E, Klemens O, Schwindt S, Becher P, Tautz N.** 2012. Pestivirus virion morphogenesis in the absence of uncleaved nonstructural protein 2-3. J. Virol. **86:**427–437. http://dx.doi.org/10.1128/JVI.06133-11.
57. **Willett R, Kudlyk T, Pokrovskaya I, Schonherr R, Ungar D, Duden R, Lupashin V.** 2013. COG complexes form spatial landmarks for distinct SNARE complexes. Nat. Commun. **4:**1553. http://dx.doi.org/10.1038/ncomms2535.
58. **Schneider CA, Rasband WS, Eliceiri KW.** 2012. NIH Image to ImageJ: 25 years of image analysis. Nat. Methods **9:**671–675. http://dx.doi.org/10.1038/nmeth.2089.
59. **Wootton JC, Federhen S.** 1996. Analysis of compositionally biased regions in sequence databases. Methods Enzymol. **266:**554–571. http://dx.doi.org/10.1016/S0076-6879(96)66035-2.
60. **Cuff JA, Barton GJ.** 1999. Evaluation and improvement of multiple sequence methods for protein secondary structure prediction. Proteins **34:**508–519.
61. **Tautz N, Meyers G, Stark R, Dubovi EJ, Thiel H-J.** 1996. Cytopathogenicity of a pestivirus correlates with a 27-nucleotide insertion. J. Virol. **70:**7851–7858.
62. **Suzuki M, Shinohara Y, Ohsaki Y, Fujimoto T.** 2011. Lipid droplets: size matters. J. Electron Microsc. **60**(Suppl 1):S101–S116. http://dx.doi.org/10.1093/jmicro/dfr016.

63. **Greenberg AS, Egan JJ, Wek SA, Garty NB, Blanchette-Mackie EJ, Londos C.** 1991. Perilipin, a major hormonally regulated adipocyte-specific phosphoprotein associated with the periphery of lipid storage droplets. J. Biol. Chem. **266:**11341–11346.
64. **Lackner T, Müller A, Pankraz A, Becher P, Thiel H-J, Gorbalenya AE, Tautz N.** 2004. Temporal modulation of an autoprotease is crucial for replication and pathogenicity of an RNA virus. J. Virol. **78:**10765–10775. http://dx.doi.org/10.1128/JVI.78.19.10765-10775.2004.
65. **Lackner T, Thiel H-J, Tautz N.** 2006. Dissection of a viral autoprotease elucidates a function of a cellular chaperone in proteolysis. Proc. Natl. Acad. Sci. U. S. A. **103:**1510–1515. http://dx.doi.org/10.1073/pnas.0508247103.
66. **Appel N, Zayas M, Miller S, Krijnse-Locker J, Schaller T, Friebe P, Kallis S, Engel U, Bartenschlager R.** 2008. Essential role of domain III of nonstructural protein 5A for hepatitis C virus infectious particle assembly. PLoS Pathog. **4:**e1000035. http://dx.doi.org/10.1371/journal.ppat.1000035.
67. **Ross-Thriepland D, Amako Y, Harris M.** 2013. The C terminus of NS5A domain II is a key determinant of hepatitis C virus genome replication, but is not required for virion assembly and release. J. Gen. Virol. **94:**1009–1018. http://dx.doi.org/10.1099/vir.0.050633-0.
68. **Hughes M, Gretton S, Shelton H, Brown DD, McCormick CJ, Angus AG, Patel AH, Griffin S, Harris M.** 2009. A conserved proline between domains II and III of hepatitis C virus NS5A influences both RNA replication and virus assembly. J. Virol. **83:**10788–10796. http://dx.doi.org/10.1128/JVI.02406-08.
69. **Hughes M, Griffin S, Harris M.** 2009. Domain III of NS5A contributes to both RNA replication and assembly of hepatitis C virus particles. J. Gen. Virol. **90:**1329–1334. http://dx.doi.org/10.1099/vir.0.009332-0.
70. **Shavinskaya A, Boulant S, Penin F, McLauchlan J, Bartenschlager R.** 2007. The lipid droplet binding domain of hepatitis C virus core protein is a major determinant for efficient virus assembly. J. Biol. Chem. **282:**37158–37169. http://dx.doi.org/10.1074/jbc.M707329200.
71. **Targett-Adams P, Hope G, Boulant S, McLauchlan J.** 2008. Maturation of hepatitis C virus core protein by signal peptide peptidase is required for virus production. J. Biol. Chem. **283:**16850–16859. http://dx.doi.org/10.1074/jbc.M802273200.
72. **Vogt DA, Camus G, Herker E, Webster BR, Tsou CL, Greene WC, Yen TS, Ott M.** 2013. Lipid droplet-binding protein TIP47 regulates hepatitis C virus RNA replication through interaction with the viral NS5A protein. PLoS Pathog. **9:**e1003302. http://dx.doi.org/10.1371/journal.ppat.1003302.
73. **Riedel C, Lamp B, Heimann M, Konig M, Blome S, Moennig V, Schuttler C, Thiel HJ, Rumenapf T.** 2012. The core protein of classical Swine Fever virus is dispensable for virus propagation in vitro. PLoS Pathog. **8:**e1002598. http://dx.doi.org/10.1371/journal.ppat.1002598.
74. **Riedel C, Lamp B, Heimann M, Rumenapf T.** 2010. Characterization of essential domains and plasticity of the classical Swine Fever virus Core protein. J. Virol. **84:**11523–11531. http://dx.doi.org/10.1128/JVI.00699-10.